

# Special Unitary Parameterized Estimators of Rotation

Akshay Chandrasekhar

## Abstract

*This paper explores rotation estimation from the perspective of special unitary matrices. First, multiple solutions to Wahba’s problem are derived through special unitary matrices, providing linear constraints on quaternion rotation parameters. Next, from these constraints, closed-form solutions to the problem are presented for minimal cases. Finally, motivated by these results, we investigate new representations for learning rotations in neural networks. Numerous experiments validate the proposed methods.*

## 1. Introduction

3D rotations are fundamental objects ubiquitously encountered in domains such as physics, aerospace, and robotics. Many representations have been developed over the years to describe them including rotation matrices, Euler angles, and quaternions. Each method has specific strengths such as parameter efficiency, singularity avoidance, or interpretability. While special orthogonal matrices  $SO(3)$  are widely used, their complex counterparts, special unitary matrices  $SU(2)$ , are less explored in areas like robotics and computer vision. This paper showcases the utility of special unitary matrices by tackling rotation estimation from different perspectives.

### 1.1. Wahba’s Problem

Wahba’s problem is a fundamental problem in attitude estimation introduced in 1965 by its namesake Grace Wahba [23]. The task refers to the process of determining the orientation of a target coordinate frame relative to a reference coordinate frame based on 3D unit vector observations. More formally, it is phrased as seeking the optimal rotation matrix  $\mathbf{R}$  that minimizes the following loss:

$$\min_{\mathbf{R} \in SO(3)} \sum_i w_i \|\mathbf{b}_i - \mathbf{R}\mathbf{a}_i\|^2 \quad (1)$$

where  $\mathbf{a}_i$  are the reference frame observations,  $\mathbf{b}_i$  are the corresponding target frame observations, and  $w_i$  are the real positive weights for each observation pair. The problem can be solved analytically by finding the nearest special orthog-

onal matrix (in a Frobenius sense) to the matrix  $\mathbf{B}$  below:

$$\mathbf{B} = \sum_i w_i \mathbf{b}_i \mathbf{a}_i^T \quad (2)$$

Today, this solution is typically computed via singular value decomposition [15].

Alternatively, the solution can be estimated as a unit quaternion. Davenport introduced the first such method in 1968 [3] by showing that the optimal quaternion  $\mathbf{q}$  is the eigenvector corresponding to the largest eigenvalue of a  $4 \times 4$  symmetric gain matrix  $\mathbf{K}$ , which can be constructed as:

$$\mathbf{K} = \begin{bmatrix} Tr(\mathbf{B}) & \mathbf{z}^T \\ \mathbf{z} & \mathbf{B} + \mathbf{B}^T - Tr(\mathbf{B})\mathbf{I} \end{bmatrix} \quad (3)$$

where  $\mathbf{I}$  is the identity matrix,  $Tr(\mathbf{B}) = \sum_i \mathbf{B}_{ii}$ , and  $\mathbf{z} = \sum_i w_i \mathbf{a}_i \times \mathbf{b}_i$ . The solution via eigendecomposition is relatively slow as it solves for all the eigenvectors of the matrix which are not needed. Later solutions improve upon this by calculating the characteristic equation of  $\mathbf{K}$  and solving for only the largest eigenvalue [18, 22, 25]. For an overview of major algorithms, see [10].

### 1.2. Representations for Learning Rotations

In recent years, there has been great interest in representing rotations within neural networks which often struggle with learning structured outputs. Directly predicting common parameterizations such as quaternions or Euler angles has generally performed poorly [4]. In fact, it was shown that any 3D rotation parameterization in less than five real dimensions is discontinuous, necessitating non-minimal representations for smooth learning [26]. Additionally, challenges like double cover in some representations can further hinder learning. Two leading approaches [8, 21] essentially interpret network outputs as the  $\mathbf{B}$  and  $\mathbf{K}$  matrices (Eqs. (2) and (3) respectively), mapping them to rotations via solutions to Wahba’s problem. Thus, the two tasks can be linked. For a detailed overview, see [4].

### 1.3. Mathematical Background

The mathematical background for special unitary matrices and related concepts is briefly reviewed. A complex square matrix  $\mathbf{U}$  is defined as unitary if:

$$\mathbf{U}\mathbf{U}^H = \mathbf{U}^H\mathbf{U} = \mathbf{I}, \quad |\det(\mathbf{U})| = 1 \quad (4)$$

where  $^H$  denotes the conjugate transpose and  $|\cdot|$  is the complex magnitude. The matrix is *special unitary* if it has the additional restriction that  $\det(\mathbf{U}) = 1$  exactly.

Stereographic projection  $\psi$  is an invertible mapping of the sphere  $S^2 = \{(x_s, y_s, z_s) \mid x_s^2 + y_s^2 + z_s^2 = 1\}$  from the point  $\mathbf{p}^* = (0, 0, -1)$  to the complex plane and is given by:

$$\begin{aligned} \psi(\mathbf{a}) &: \frac{x_s}{1+z_s} + \frac{y_s}{1+z_s}i = x_p + y_pi = z \quad (5) \\ \psi^{-1}(z) &: \left( \frac{2x_p}{1+x_p^2+y_p^2}, \frac{2y_p}{1+x_p^2+y_p^2}, \frac{1-x_p^2-y_p^2}{1+x_p^2+y_p^2} \right) \quad (6) \end{aligned}$$

where  $\mathbf{a} \in S^2$  and  $z \in \mathbb{C}$ . Note that  $\psi$  is undefined when  $\mathbf{a} = \mathbf{p}^*$ . To overcome this, the map is extended to the complex projective space which includes the point at infinity so we can define  $\psi(\mathbf{p}^*) = \infty$ . The projection is now redefined below with equivalence relations:

$$\begin{aligned} \psi(\mathbf{a}) &\mapsto \begin{cases} \begin{bmatrix} z \\ 1 \end{bmatrix} \sim \lambda \begin{bmatrix} z \\ 1 \end{bmatrix}, & \mathbf{a} \neq \mathbf{p}^* \\ \infty \sim \begin{bmatrix} \lambda \\ 0 \end{bmatrix}, & \mathbf{a} = \mathbf{p}^* \end{cases} \quad (7) \\ \lambda \in \mathbb{C}, \lambda \neq 0, \psi^{-1}(\psi(\mathbf{a})) &= \mathbf{a} \end{aligned}$$

so  $\psi(\mathbf{a})$  can be arbitrarily scaled, and  $\psi$  bijectively maps the entire sphere to the complex projective space. Note that this mapping is not unique, particularly since choice of  $\mathbf{p}^*$  is arbitrary. We will use the specific projection defined above for this paper as it is convenient for image processing.

A special unitary matrix  $\mathbf{U} \in SU(2)$  can generally be written as:

$$\begin{aligned} \mathbf{U} &= \begin{bmatrix} \alpha & \beta \\ -\bar{\beta} & \bar{\alpha} \end{bmatrix} \quad (8) \\ \alpha\bar{\alpha} + \beta\bar{\beta} &= 1, \alpha, \beta \in \mathbb{C} \end{aligned}$$

$\mathbf{U}$  transforms a complex projective point  $\mathbf{z} = [z_1, z_2]^T$  and complex plane point  $z$  by:

$$\mathbf{U} : \mathbf{z} \mapsto \mathbf{z}' = \mathbf{U}\mathbf{z} = \begin{bmatrix} \alpha & \beta \\ -\bar{\beta} & \bar{\alpha} \end{bmatrix} \begin{bmatrix} z_1 \\ z_2 \end{bmatrix} \quad (9)$$

$$\Phi_{\mathbf{U}} : z \mapsto z' = \frac{\alpha z + \beta}{-\bar{\beta}z + \bar{\alpha}}, \quad -\bar{\beta}z + \bar{\alpha} \neq 0 \quad (10)$$

These transformations are of importance as they act analogously to rotations of the unit sphere in  $\mathbb{R}^3$ . Specifically, for a 3x3 rotation matrix  $\mathbf{R} \in SO(3)$  that rotates a unit vector  $\mathbf{v} \in S^2$  as  $\mathbf{v}' = \mathbf{R}\mathbf{v}$ , there exists some  $\mathbf{U}$  such that:

$$\mathbf{v}' = (\psi^{-1} \circ \mathbf{U} \circ \psi)(\mathbf{v}) \quad (11)$$

The exact relationship between  $SU(2)$  and  $SO(3)$  is made clearer by their relationships with unit quaternions

$\mathbf{q} \in \mathbb{H}$  which also act as rotations in  $\mathbb{R}^3$ . The isomorphism between  $SU(2)$  and unit quaternions is given as:

$$\begin{aligned} \mathbf{q} &= w_q + x_qi + y_qj + z_qk \\ w_q^2 + x_q^2 + y_q^2 + z_q^2 &= 1, \quad w_q, x_q, y_q, z_q \in \mathbb{R} \\ \alpha &= w_q + x_qi, \quad \beta = y_q + z_qi \quad (12) \end{aligned}$$

and the mapping of unit quaternions to special orthogonal matrices is given by:

$$\mathbf{R}_{\mathbf{q}} = \begin{bmatrix} 1 - 2y_q^2 - 2z_q^2 & 2x_qy_q - 2w_qz_q & 2x_qz_q + 2w_qy_q \\ 2x_qy_q + 2w_qz_q & 1 - 2x_q^2 - 2z_q^2 & 2y_qz_q - 2w_qx_q \\ 2x_qz_q - 2w_qy_q & 2y_qz_q + 2w_qx_q & 1 - 2x_q^2 - 2y_q^2 \end{bmatrix} \quad (13)$$

Eq. (13) is the well-known 2-to-1 surjective mapping between quaternions and rotation matrices. By their isomorphism in Eq. (12),  $SU(2)$  also has a similar surjective mapping with  $SO(3)$ , linking the three rotation representations. Note that the mapping given by Eq. (12) is not unique.

Furthermore, special unitary matrices have the ability to act as rotations in  $\mathbb{R}^3$  directly by first mapping points to 2x2 complex matrices. For a point  $\mathbf{x} = (x, y, z) \in \mathbb{R}^3$ :

$$\chi : \mathbf{x} \mapsto \mathbf{X} = \begin{bmatrix} xi & y + zi \\ -y + zi & -xi \end{bmatrix} \quad (14)$$

$$\begin{aligned} \chi(\mathbf{x}_1) &\mapsto \mathbf{X}_1, \quad \chi(\mathbf{x}_2) \mapsto \mathbf{X}_2, \quad \mathbf{x}_1, \mathbf{x}_2 \in \mathbb{R}^3 \\ \mathbf{X}_2 &= \mathbf{U}\mathbf{X}_1\mathbf{U}^H, \quad \mathbf{U} \in SU(2) \quad (15) \end{aligned}$$

Note if  $\|\mathbf{x}\| = 1$ ,  $\chi(\mathbf{x}) \in SU(2)$ . Also note that the map  $\chi$  is not uniquely defined either.

Relatedly, Möbius transformations are general 2x2 complex projective matrices, characterized similarly by:

$$\begin{aligned} \mathbf{M} &= \begin{bmatrix} \sigma & \xi \\ \gamma & \delta \end{bmatrix} \quad (16) \\ \sigma, \xi, \gamma, \delta \in \mathbb{C}, \det(\mathbf{M}) &\neq 0, \mathbf{M} \in PGL(2, \mathbb{C}) \end{aligned}$$

$$\mathbf{M} : \mathbf{z} \mapsto \mathbf{z}' = \mathbf{M}\mathbf{z} = \begin{bmatrix} \sigma & \xi \\ \gamma & \delta \end{bmatrix} \begin{bmatrix} z_1 \\ z_2 \end{bmatrix} \quad (17)$$

$$\Phi_{\mathbf{M}} : z \mapsto z' = \frac{\sigma z + \xi}{\gamma z + \delta}, \quad \gamma z + \delta \neq 0 \quad (18)$$

$$\mathbf{M} \sim \lambda\mathbf{M}, \quad \lambda \in \mathbb{C}, \lambda \neq 0 \quad (19)$$

Möbius transformations conformally map the complex projective plane onto itself. They are uniquely determined (up to scale) by their action on three independent points, and  $SU(2)$  elements constitute a subset of them.

## 2. Solutions to Wahba's Problem via $SU(2)$

In this section, we transfer Wahba's Problem to complex projective space and solve for the optimal rotation as a special unitary matrix. We motivate this by noting that rotation matrices act linearly in  $\mathbb{R}^3$ , but have several nontrivial

constraints to enforce. Quaternions have a single constraint to enforce (unit norm), but act quadratically in  $\mathbb{R}^3$  as seen from Eq. (13). Interestingly, Eqs. (9) and (10) show us that through special unitary matrices, quaternion parameters act linearly in the complex projective space— an insight that we exploit below.

## 2.1. Stereographic Plane Solution

First, we establish the proper distance metric in complex projective space corresponding to the spherical chordal metric in Eq. (1). For points  $\mathbf{a}, \mathbf{b} \in S^2$  and complex projective points  $\psi(\mathbf{a}) = \mathbf{z} = [z_1, z_2]^T$  and  $\psi(\mathbf{b}) = \mathbf{p} = [p_1, p_2]^T$ , we can show that the metric can be expressed in the following way (proof in Suppl. Mat.):

$$\|\mathbf{a} - \mathbf{b}\|^2 = \frac{4|z_1 p_2 - z_2 p_1|^2}{\|\mathbf{z}\|^2 \|\mathbf{p}\|^2} \quad (20)$$

We now seek to find the rotation  $\mathbf{R}$  parameterized by special unitary matrix  $\mathbf{U}$  that minimizes the objective in Eq. (1). Applying our derived metric and Eq. (9), we can construct for each weighted input correspondence  $\mathbf{z}_i$  and  $\mathbf{p}_i$ :

$$\begin{aligned} & w_i \|\mathbf{b}_i - \mathbf{R}\mathbf{a}_i\|^2 \\ &= \frac{4w_i |(-\bar{\beta}z_{i,1} + \bar{\alpha}z_{i,2})p_{i,1} - (\alpha z_{i,1} + \beta z_{i,2})p_{i,2}|^2}{(|\alpha z_{i,1} + \beta z_{i,2}|^2 + |-\bar{\beta}z_{i,1} + \bar{\alpha}z_{i,2}|^2) \|\mathbf{p}_i\|^2} \\ &= \frac{4w_i |(-\bar{\beta}z_{i,1} + \bar{\alpha}z_{i,2})p_{i,1} - (\alpha z_{i,1} + \beta z_{i,2})p_{i,2}|^2}{\|\mathbf{U}\mathbf{z}_i\|^2 \|\mathbf{p}_i\|^2} \end{aligned}$$

By definition of unitary matrices,  $\|\mathbf{U}\mathbf{z}_i\|^2 = \mathbf{z}_i^H \mathbf{U}^H \mathbf{U} \mathbf{z}_i = \|\mathbf{z}_i\|^2$ . Thus, we can rewrite our expression as the following target constraint (subscript  $i$  dropped):

$$\frac{4w |(-\bar{\beta}z_1 + \bar{\alpha}z_2)p_1 - (\alpha z_1 + \beta z_2)p_2|^2}{\|\mathbf{z}\|^2 \|\mathbf{p}\|^2} = 0 \quad (21)$$

$$\implies \frac{2\sqrt{w} ( (-\bar{\beta}z_1 + \bar{\alpha}z_2)p_1 - (\alpha z_1 + \beta z_2)p_2 )}{\sqrt{|z_1|^2 + |z_2|^2} \sqrt{|p_1|^2 + |p_2|^2}} = 0 \quad (22)$$

The expression is now just a linear function of rotation parameters. It is a general constraint as it handles the entire complex projective space. However, in practice, our inputs are more commonly given as projection coordinates on the complex plane. As such, we have:

$$\begin{aligned} z_{i,1} &= z_i = x_i + y_i i \\ p_{i,1} &= p_i = m_i + n_i i \\ z_{i,2} &= p_{i,2} = 1 \end{aligned}$$

for each point correspondence. This simplifies the previous constraint to the following:

$$\frac{2\sqrt{w_i} ( (-\bar{\beta}z_i + \bar{\alpha})p_i - \alpha z_i - \beta )}{\sqrt{|z_i|^2 + 1} \sqrt{|p_i|^2 + 1}} = 0 \quad (23)$$

We can rearrange the equation to the following linear form:

$$\mathbf{u} = [\alpha \ \beta \ \bar{\alpha} \ \bar{\beta}]^T$$

$$w'_i = \frac{4w_i}{(|z_i|^2 + 1)(|p_i|^2 + 1)} \quad (24)$$

$$\sqrt{w'_i} [-z_i \ -1 \ p_i \ -p_i z_i] \mathbf{u} = \sqrt{w'_i} \mathbf{A}_i \mathbf{u} = 0 \quad (25)$$

Each input point pair gives us a complex constraint  $\mathbf{A}_i$ . Stacking  $\mathbf{A}_i$  together and multiplying the weights through, we can write the relation succinctly as  $\mathbf{A}\mathbf{u} = 0$  ( $\mathbf{A}$  is a complex  $n \times 4$  matrix for  $n$  points). With noisy observations, the constraints do not hold exactly, so we aim to find the best rotation that minimizes the least squares error  $\|\mathbf{A}\mathbf{u}\|^2$ . It is nontrivial to solve for the minimizing vector  $\mathbf{u}$  while ensuring the result will form a valid special unitary matrix ( $\mathbf{u}_1 = \bar{\mathbf{u}}_3, \mathbf{u}_2 = \bar{\mathbf{u}}_4, \mathbf{u}_1 \bar{\mathbf{u}}_1 + \mathbf{u}_2 \bar{\mathbf{u}}_2 = 1$ ).

To more effectively solve this, we use Eq. (12) to transform the vector  $\mathbf{u}$  to a corresponding quaternion  $\mathbf{q}$  that has a simpler constraint ( $\mathbf{q}$  must be unit norm). We carry out the complex multiplication for each  $\mathbf{A}_i \mathbf{u}$  and break the constraint into two constraints, one for the real and imaginary parts respectively (subscript  $i$  partially dropped):

$$\mathbf{q} = [w_q \ x_q \ y_q \ z_q]^T$$

$$w'_i = \frac{4w_i}{(1 + x_i^2 + y_i^2)(1 + m_i^2 + n_i^2)} \quad (26)$$

$$\begin{aligned} & \sqrt{w'} \begin{bmatrix} x - m & -y - n & 1 + mx - ny & my + nx \\ y - n & x + m & my + nx & 1 - mx + ny \end{bmatrix} \mathbf{q} \\ &= \sqrt{w'_i} \mathbf{D}_i \mathbf{q} = 0 \end{aligned} \quad (27)$$

Multiplying the weights through again and stacking together  $\mathbf{D}_i$  for each correspondence into  $\mathbf{D}$  (real  $2n \times 4$  matrix), we can arrive at the following constrained least squares objective:

$$\begin{aligned} \|\mathbf{D}\mathbf{q}\|^2 &= \mathbf{q}^T \mathbf{D}^T \mathbf{D} \mathbf{q} = \mathbf{q}^T \left( \sum_i w'_i \mathbf{D}_i^T \mathbf{D}_i \right) \mathbf{q} = \mathbf{q}^T \mathbf{G}_P \mathbf{q} \\ \min_{\mathbf{q}} \mathbf{q}^T \mathbf{G}_P \mathbf{q}, \quad s.t. \quad \|\mathbf{q}\| &= 1 \end{aligned} \quad (28)$$

The formulated objective in Eq. (28) is equivalent to the original problem statement, and the solution is well known as the eigenvector corresponding to the smallest eigenvalue of  $\mathbf{G}_P$ . Using Eq. (12) again, we can map  $\mathbf{q}$  back to a special unitary matrix  $\mathbf{U}$  giving a solution to the problem. Note that  $-\mathbf{q}$  is also a solution since eigenvectors are only unique up to scale. However, the sign is irrelevant as  $\mathbf{q}$  and  $-\mathbf{q}$  map to the same rotation due to the double cover of quaternions over  $SO(3)$  in Eq. (13).

## 2.2. Recovering $\mathbf{R}$

The solution  $\mathbf{U}$  obtained precisely satisfies the relation in Eq. (11). However, using the maps laid out in Eqs. (12)

and (13) directly will lead to a rotation  $\mathbf{R}_U$  that is not necessarily equivalent to the desired  $\mathbf{R}$  in Eq. (1). This is because our choice of  $\psi$  and choice of isomorphism between quaternions and special unitary matrices can each add an implicit orthogonal transformation in their map. Since their combined transformation  $\Psi$  and its inverse are applied before and after estimation respectively, the relationship between  $\mathbf{U}$  and  $\mathbf{R}$  is characterized by the conjugate transformation:

$$\mathbf{R} = \Psi^T \mathbf{R}_U \Psi \quad (29)$$

For our definitions, we find that  $\Psi$  is simply a 90 degree rotation about the y-axis. When applied directly to the resulting  $\mathbf{q}$  from the algorithm, the transformed quaternion is given as:

$$\mathbf{q}^* = w_q - z_q i + y_q j + x_q k \quad (30)$$

which is just a permutation/negation of the elements of  $\mathbf{q}$ . We can verify that mapping  $\mathbf{q}^*$  to  $\mathbf{R}$  via Eq. (13) indeed gives us the true optimal solution to the problem.

### 2.3. Approximation via Möbius Transformations

We can approximate the previous solution in the complex domain by first estimating an optimal Möbius transformation  $\mathbf{M}$  and mapping it to a special unitary matrix. Relaxing the special unitary conditions in Eq. (25), we can treat  $\mathbf{u}$  as a flattened form of  $\mathbf{M}$ , leading to a modified constraint  $\mathbf{A}'_i$  that holds when  $\mathbf{M}$  aligns a stereographic point pair:

$$\mathbf{m} = \text{vec}(\mathbf{M}) = [\sigma \quad \xi \quad \gamma \quad \delta]^T \\ [-z_i \quad -1 \quad p_i z_i \quad p_i] \mathbf{m} = \mathbf{A}'_i \mathbf{m} = 0 \quad (31)$$

Note that Eq. (31) does not preserve the metric in Eq. (20) between  $p_i$  and transformed point  $\Phi_M(z_i)$ . We can stack each  $\mathbf{A}'_i$  into matrix  $\mathbf{A}'$  ( $n \times 4$  complex matrix) and similarly estimate the best (in a least squares sense) Möbius transformation aligning the points as:

$$\mathbf{G}_M = \mathbf{A}'^H \mathbf{A}' = \sum_i \mathbf{A}'_i{}^H \mathbf{A}'_i \\ \min_{\mathbf{m}} \mathbf{m}^H \mathbf{G}_M \mathbf{m} \quad \text{s.t.} \quad \|\mathbf{m}\| = 1 \quad (32)$$

The constraint in Eq. (32) is necessary to prevent trivial solutions, but the choice of quadratic constraint on  $\mathbf{m}$  is arbitrary. With our constraint choice, the optimal  $\mathbf{m}$  is the complex eigenvector corresponding to the smallest eigenvalue of  $\mathbf{G}_M$ . Since  $\mathbf{G}_M$  is Hermitian ( $\mathbf{G}_M^H = \mathbf{G}_M$ ) by construction, the eigenvalues are real and nonnegative, facilitating straightforward ordering. If  $n < 4$ ,  $\mathbf{m}$  can be obtained directly from the kernel of  $\mathbf{A}'$ . Either way, the solution is not unique as eigenvectors and kernel vectors can be scaled arbitrarily (particularly by a phase  $e^{i\theta}$ ). However, by Eq. (19), scaled Möbius transformations are equivalent, so our result properly defines the transformation.

Given  $\mathbf{m}$ , we can reshape it into  $\mathbf{M}$  and scale  $\mathbf{M}$  to  $\mathbf{M}^* = \det(\mathbf{M})^{-\frac{1}{2}} \mathbf{M}$  (allowed since the scale of  $\mathbf{M}$  is arbitrary) so that  $\det(\mathbf{M}^*) = 1$ . It is known that the closest unitary matrix to  $\mathbf{M}^*$  in the Frobenius sense can be computed by  $\mathbf{U}\mathbf{V}^H$  [6], where  $\mathbf{U}$  and  $\mathbf{V}^H$  are from the singular value decomposition  $\mathbf{M}^* = \mathbf{U}\Sigma\mathbf{V}^H$ . Since  $\det(\mathbf{M}^*) = 1$ , the nearest unitary matrix to  $\mathbf{M}^*$  is in fact special unitary (Proof in Supp. Mat.) and is thus the approximate solution. Note that this matrix is not necessarily the nearest special unitary matrix to  $\mathbf{M}$  itself. By normalizing the determinant, we prevent the rotation mapping from being affected by arbitrary phase scalings of  $\mathbf{m}$ .

### 2.4. 3D Sphere Solution

If our inputs are given as unit observations in 3D, we could project them by  $\psi$  and use the earlier solution. However, through Eqs. (14) and (15), we see that we can act directly on 3D vectors with special unitary matrices which suggests an alternative formulation. Upon examining the structure of the matrices that  $\chi$  maps to, one can show that Eq. (1) can be equivalently expressed as:

$$\chi(\mathbf{a}_i) \mapsto \mathbf{Z}_i, \quad \chi(\mathbf{b}_i) \mapsto \mathbf{P}_i \\ \sum_i w_i \|\mathbf{b}_i - \mathbf{R}\mathbf{a}_i\|^2 = \frac{1}{2} \sum_i w_i \|\mathbf{P}_i - \mathbf{U}\mathbf{Z}_i\mathbf{U}^H\|_F^2 \quad (33)$$

where  $\|\cdot\|_F$  denotes the Frobenius norm and  $\mathbf{U}$  is the special unitary matrix that maps to  $\mathbf{R}$ . The Frobenius norm is unitarily invariant, so we may multiply the inside expression on the right by  $\mathbf{U}$  to obtain a new objective and corresponding constraint:

$$\frac{1}{2} \sum_i w_i \|\mathbf{P}_i \mathbf{U} - \mathbf{U}\mathbf{Z}_i\|_F^2 \quad (34)$$

$$\sqrt{\frac{w_i}{2}} (\mathbf{P}_i \mathbf{U} - \mathbf{U}\mathbf{Z}_i) = 0 \quad (35)$$

We arrive at a linear constraint again via special unitary matrices. Inspecting the matrix within the Frobenius norm reveals that the loss contribution from the top row elements is identical to that of the bottom row elements. Consequently, we only need to compute the loss from a single row, allowing us to eliminate the factor of  $\frac{1}{2}$  from equation Eq. (35). With  $\mathbf{a}_i = (x_i, y_i, z_i)$  and  $\mathbf{b}_i = (m_i, n_i, p_i)$ , we can write the following complex constraint (subscript  $i$  partially dropped):

$$\sqrt{w} \begin{bmatrix} (m-x)i & y-zi & 0 & -n-pi \\ -y-zi & (x+m)i & n+pi & 0 \end{bmatrix} \mathbf{u} \\ = \sqrt{w}_i \mathbf{C}_i \mathbf{u} = 0 \quad (36)$$

$\mathbf{C}_i$  has a rank of at most 1 if  $\mathbf{a}$  and  $\mathbf{b}$  have the same magnitude. We reformulate the constraint, once again breaking

the complex terms of  $\mathbf{u}$  into their real components. This yields the following linear constraint in terms of quaternion parameters (subscript  $i$  partially dropped):

$$\sqrt{w} \begin{bmatrix} 0 & x-m & y-n & z-p \\ m-x & 0 & -z-p & y+n \\ n-y & z+p & 0 & -x-m \\ p-z & -y-n & x+m & 0 \end{bmatrix} \mathbf{q} = \sqrt{w_i} \mathbf{Q}_i \mathbf{q} = 0 \quad (37)$$

Note that  $\mathbf{Q}_i$  is a 4x4 skew-symmetric matrix and has at most rank 2 if  $\mathbf{a}$  and  $\mathbf{b}$  have the same magnitude. As a result, our optimization now becomes:

$$\sum_i w_i \mathbf{Q}_i^T \mathbf{Q}_i = - \sum_i w_i \mathbf{Q}_i^2 = \mathbf{G}_S \quad (38)$$

$$\min_{\mathbf{q}} \mathbf{q}^T \mathbf{G}_S \mathbf{q} \quad s.t. \quad \|\mathbf{q}\| = 1$$

The solution is once again the eigenvector corresponding to the smallest eigenvalue of  $\mathbf{G}_S$ .

### 3. Rotations of Exact Alignment

When the constraints of Eqs. (27) and (37) hold exactly, the solution can be obtained more simply. This section explores those cases and their applications for 3D unit vector inputs. Similar formulas can be derived for stereographic inputs.

#### 3.1. One-Point Case

Finding a rotation that aligns two unit vectors (*i.e.*  $\mathbf{b} = \mathbf{R}\mathbf{a}$ ) is a special case of Wahba's problem where  $n = 1$ . Since aligning a pair of points constrains two out of three rotational degrees of freedom ( $\mathbf{D}_i$  and  $\mathbf{Q}_i$  have rank 2), there are infinite solutions in this case. The rotation whose axis is the cross product of the points is often chosen for geometric simplicity and can be calculated efficiently as:

$$s = \sqrt{2(1 + \mathbf{a} \cdot \mathbf{b})}$$

$$\mathbf{q} = \left( \frac{s}{2}, \frac{\mathbf{a} \times \mathbf{b}}{s} \right) \quad (39)$$

Instead, we may choose another convention where we constrain an element of the quaternion to be 0.

Since the points can be perfectly aligned,  $\mathbf{q}^T \mathbf{G}_S \mathbf{q} = 0$ , so  $\mathbf{q} \in \text{Null}(\mathbf{Q}_i)$ . Leveraging this fact, we can simply take two linearly independent rows from  $\mathbf{Q}_i$  and set them to 0 explicitly, imposing a rank 2 constraint. Given the homogeneous nature of this system, we can disregard the weight and determine the rotation using straightforward linear algebra techniques. Each row below is a member of the kernel that has a quaternion element equal to 0 (note only two rows are linearly independent):

$$\left\{ \begin{array}{cccc} 0 & x+m & y+n & z+p \\ x+m & 0 & z-p & n-y \\ y+n & p-z & 0 & x-m \\ z+p & y-n & m-x & 0 \end{array} \right\} \in \ker(\mathbf{Q}_i) \quad (40)$$

Normalizing any nonzero row of Eq. (40) gives an optimal rotation. Compared to Eq. (39), this approach has several advantages. First, the rotation is simpler to construct. Second, one of its elements is guaranteed to be 0, so composing rotations and rotating points requires fewer operations and memory accesses. This is particularly true for the first row of Eq. (40) as it represents a 180 degree rotation whose action on a point can be more efficiently computed as a reflection about an axis. Finally, Eq. (39) has a singularity when the cross product vanishes. Although each row of Eq. (40) has its own singular region, it is straightforward to systematically select another row that is well-defined in that region.

#### 3.2. Noiseless Two-Point Case

With two independent sets of correspondences, we are able to fully constrain the rotation to a unique one. If we assume that the two sets can be aligned perfectly, then we can recover an optimal rotation from the intersection of the constraint kernels.

Two independent rows of Eq. (40) can be basis vectors for the kernel of  $\mathbf{Q}_1$ . We can determine the optimal rotation by finding the member of  $\ker(\mathbf{Q}_1)$  (represented as a linear combination of basis vectors) that is orthogonal to an independent row of  $\mathbf{Q}_2$ . For example, with the last two rows of Eq. (40) as a basis of  $\mathbf{Q}_1$  and the first row of  $\mathbf{Q}_2$ :

$$\begin{bmatrix} 0 \\ x_2 - m_2 \\ y_2 - n_2 \\ z_2 - p_2 \end{bmatrix} \cdot \left( a \begin{bmatrix} z_1 + p_1 \\ y_1 - n_1 \\ m_1 - x_1 \\ 0 \end{bmatrix} + b \begin{bmatrix} y_1 + n_1 \\ p_1 - z_1 \\ 0 \\ x_1 - m_1 \end{bmatrix} \right) = 0$$

$$a = (x_2 - m_2)(z_1 - p_1) + (z_2 - p_2)(m_1 - x_1)$$

$$b = (x_2 - m_2)(y_1 - n_1) + (y_2 - n_2)(m_1 - x_1)$$

Substituting  $a$  and  $b$  back into the linear combination and dividing by  $m_1 - x_1$  gives the following result:

$$\tilde{\mathbf{q}} = \begin{bmatrix} (\mathbf{a}_1 + \mathbf{b}_1) \cdot (\mathbf{a}_2 - \mathbf{b}_2) \\ (\mathbf{a}_1 - \mathbf{b}_1) \times (\mathbf{a}_2 - \mathbf{b}_2) \end{bmatrix} \quad (41)$$

where  $\tilde{\mathbf{q}}$  denotes the unnormalized quaternion. This result is equivalent to the simple estimators found in [2, 16]. However, an issue with this approach is that the singular region of this estimator is not simple, and the equation fails to produce a valid rotation under several conditions (see [20]). Rather than checking each condition with a threshold or applying sequential rotations to avoid these cases like other kernel methods, we can more systematically select the three vectors in our computation to guarantee a valid result.

In general, we observe that for a point pair, either  $\mathbf{a} + \mathbf{b}$  or  $\mathbf{a} - \mathbf{b}$  will have at least one significantly nonzero element. We can select the two rows from Eq. (40) corresponding to a nonzero element from these vectors for the first point pair to ensure linearly independent kernel vectors. We then choose

one of the two rows of  $\mathbf{Q}_2$  corresponding to a nonzero element of  $\mathbf{a} + \mathbf{b}$  or  $\mathbf{a} - \mathbf{b}$  for the second point pair to solve for the rotation. For instance, if  $x_1 + m_1 \neq 0$  and  $y_2 + n_2 \neq 0$ , we can choose the first two rows of Eq. (40) and the last row of  $\mathbf{Q}_2$  to produce another equation for the rotation:

$$\begin{aligned} \mathbf{k}_1 &= [p_1 - z_1 \quad -y_1 - n_1 \quad x_1 + m_1]^T \\ \mathbf{k}_2 &= [z_1 + p_1 \quad y_1 - n_1 \quad m_1 - x_1]^T \\ \mathbf{k}_3 &= [p_2 - z_2 \quad -y_2 - n_2 \quad x_2 + m_2]^T \\ \tilde{\mathbf{q}} &= \begin{bmatrix} \mathbf{k}_1 \times \mathbf{k}_3 \\ \mathbf{k}_2 \cdot \mathbf{k}_3 \end{bmatrix} \end{aligned} \quad (42)$$

Though the dot and cross products are in different indices from before, the formulation is equally simple to compute. We select the nonzero elements by largest magnitude for robustness. At least one of the two rows we select from  $\mathbf{Q}_2$  will yield a valid rotation for  $\mathbf{a}_1 \times \mathbf{a}_2 \neq 0$ . Otherwise, the rotation is a kernel vector of  $\mathbf{Q}_1$ . We verify row validity by checking if either coefficient  $a$  or  $b$  for the relevant constraints is nonzero. Those coefficients are always reused in the final rotation calculation (*e.g.*  $a$  and  $b$  are the second and first elements respectively in Eq. (42)). This process therefore covers the whole domain and only requires a handful of operations and comparisons even in the worst case.

### 3.3. General Two-Point Case

The previous method can be applied in optimally aligning two point sets when perfect alignment is not possible (*i.e.* Wahba's problem for  $n = 2$ ). This scenario is well known to have closed-form expressions [13, 18, 22]. We propose an alternate solution given by the average of two (unnormalized) rotations that each perfectly align the cross products of the reference and target sets, along with one of the two corresponding observation pairs (proof in Suppl. Mat.). Using the average rotation definition from [14], the solution is:

$$\begin{aligned} \mathbf{n}_1 &= \mathbf{a}_1 \times \mathbf{a}_2, \quad \mathbf{n}_2 = \sqrt{\frac{\|\mathbf{a}_1 \times \mathbf{a}_2\|^2}{\|\mathbf{b}_1 \times \mathbf{b}_2\|^2}} (\mathbf{b}_1 \times \mathbf{b}_2) \\ \tilde{\mathbf{q}}_i &= \begin{bmatrix} (\mathbf{a}_i + \mathbf{b}_i) \cdot (\mathbf{n}_1 - \mathbf{n}_2) \\ (\mathbf{a}_i - \mathbf{b}_i) \times (\mathbf{n}_1 - \mathbf{n}_2) \end{bmatrix} \\ \tau &= (w_1 - w_2) \|\tilde{\mathbf{q}}_1\|^2 \|\tilde{\mathbf{q}}_2\|^2, \quad \omega = 2w_1 \|\tilde{\mathbf{q}}_2\|^2 (\tilde{\mathbf{q}}_1 \cdot \tilde{\mathbf{q}}_2) \\ \nu &= 2w_2 \|\tilde{\mathbf{q}}_1\|^2 (\tilde{\mathbf{q}}_1 \cdot \tilde{\mathbf{q}}_2), \quad \mu = \tau + \sqrt{\tau^2 + \omega\nu} \\ \mathbf{q} &= \frac{\mu \tilde{\mathbf{q}}_1 + \nu \tilde{\mathbf{q}}_2}{\sqrt{\|\tilde{\mathbf{q}}_1\|^2 \mu^2 + \|\tilde{\mathbf{q}}_2\|^2 \nu^2 + 2(\tilde{\mathbf{q}}_1 \cdot \tilde{\mathbf{q}}_2) \mu \nu}} \end{aligned} \quad (43)$$

where  $\tilde{\mathbf{q}}_1 \cdot \tilde{\mathbf{q}}_2$  denotes the usual vector dot product between  $\tilde{\mathbf{q}}_1$  and  $\tilde{\mathbf{q}}_2$ . See Suppl. Mat. for derivation and details.

In the general case of  $w_1 = w_2$  (*i.e.* unweighted case), the optimal rotation simplifies to the rotation which perfectly aligns  $\mathbf{a}_1 + \mathbf{a}_2$  to  $\mathbf{b}_1 + \mathbf{b}_2$  and  $\mathbf{a}_1 - \mathbf{a}_2$  to  $\mathbf{b}_1 - \mathbf{b}_2$

(proof in Suppl. Mat.). This is given by:

$$\begin{aligned} \mathbf{s}_1 &= \mathbf{a}_1 + \mathbf{a}_2, \quad \mathbf{s}_2 = \sqrt{\frac{1 + \mathbf{a}_1 \cdot \mathbf{a}_2}{1 + \mathbf{b}_1 \cdot \mathbf{b}_2}} (\mathbf{b}_1 + \mathbf{b}_2) \\ \mathbf{d}_1 &= \mathbf{a}_1 - \mathbf{a}_2, \quad \mathbf{d}_2 = \sqrt{\frac{1 - \mathbf{a}_1 \cdot \mathbf{a}_2}{1 - \mathbf{b}_1 \cdot \mathbf{b}_2}} (\mathbf{b}_1 - \mathbf{b}_2) \\ \tilde{\mathbf{q}} &= \begin{bmatrix} (\mathbf{s}_1 + \mathbf{s}_2) \cdot (\mathbf{d}_1 - \mathbf{d}_2) \\ (\mathbf{s}_1 - \mathbf{s}_2) \times (\mathbf{d}_1 - \mathbf{d}_2) \end{bmatrix} \end{aligned} \quad (44)$$

The aligning rotation formulas are given in the form of equation Eq. (41) for simplicity, but in practice we use the approach described in Sec. 3.2 for robustness. Singular cases only arise when  $\mathbf{a}_1 \times \mathbf{a}_2 = 0$  or  $\mathbf{b}_1 \times \mathbf{b}_2 = 0$  where no unique solution exists, and a particular one may be obtained via the special unitary constraints in equation Eq. (36) (details in Suppl. Mat.). Notably, the two solutions above are optimal in the sense of Wahba's problem and simplified compared to existing two-point methods, especially for the unweighted case.

## 4. Representations for Learning Rotations

Based on the previous sections, we introduce two higher-dimensional representations for learning rotations. The first is based on our formula for optimal rotation from two unweighted observations and is denoted **2-vec**. Similar to the Gram-Schmidt map in [26], 2-vec interprets a 6D output vector from a model as target 3D  $x$  and  $y$  axes (denoted  $\mathbf{b}_x, \mathbf{b}_y$ ). Unlike the Gram-Schmidt method which greedily orthogonalizes the two vectors by assuming the  $x$ -axis prediction is correct, 2-vec maps the two vectors to a rotation optimally in the sense of Wahba's problem, balancing error from both axis predictions. Eq. (44) could be used, but since the reference points are the  $x, y$  coordinate axes and  $\mathbf{b}_x, \mathbf{b}_y$  are unnormalized, we can instead obtain a rotation matrix in a simpler fashion through the same principle:

$$\begin{aligned} \mathbf{b}'_y &= \frac{\|\mathbf{b}_x\|}{\|\mathbf{b}_y\|} \mathbf{b}_y, \quad \mathbf{b}^+ = \frac{\mathbf{b}_x + \mathbf{b}'_y}{\|\mathbf{b}_x + \mathbf{b}'_y\|}, \quad \mathbf{b}^- = \frac{\mathbf{b}_x - \mathbf{b}'_y}{\|\mathbf{b}_x - \mathbf{b}'_y\|} \\ \mathbf{R} &= \left[ \frac{1}{\sqrt{2}} (\mathbf{b}^+ + \mathbf{b}^-), \quad \frac{1}{\sqrt{2}} (\mathbf{b}^+ - \mathbf{b}^-), \quad \mathbf{b}^- \times \mathbf{b}^+ \right] \end{aligned} \quad (45)$$

A second parameterization is based on the approximation from Sec. 2.3 involving Möbius transformations. Taking inspiration from the approach in [21], a (real) 16D network output  $\Theta = \{\theta_i : i = 1 \dots 16\}$  is arranged into the unique complex elements of  $\mathbf{G}_M$  as below:

$$\mathbf{G}_M(\Theta) = \begin{bmatrix} \theta_1 & \theta_2 + \theta_3 i & \theta_4 + \theta_5 i & \theta_6 + \theta_7 i \\ \theta_2 - \theta_3 i & \theta_8 & \theta_9 + \theta_{10} i & \theta_{11} + \theta_{12} i \\ \theta_4 - \theta_5 i & \theta_9 - \theta_{10} i & \theta_{13} & \theta_{14} + \theta_{15} i \\ \theta_6 - \theta_7 i & \theta_{11} - \theta_{12} i & \theta_{14} - \theta_{15} i & \theta_{16} \end{bmatrix} \quad (46)$$

$\mathbf{G}_M(\Theta)$  is Hermitian with real (and assumed distinct) eigenvalues where we can select the eigenvector  $\mathbf{m}$  corresponding to its smallest eigenvalue. After reshaping  $\mathbf{m}$  to a

Möbius transformation  $\mathbf{M}$ , we can map to a rotation by the approximation procedure in Sec. 2.3. The procedure can be performed via linear algebra techniques to obtain a special unitary matrix  $\mathbf{Q}$  that can be mapped to a quaternion by Eqs. (12) and (30):

$$\mathbf{M} = \mathbf{U}\Sigma\mathbf{V}^H$$

$$\mathbf{Q} = \sqrt{\det(\mathbf{U}\mathbf{V}^H)}\mathbf{U}\mathbf{V}^H \in SU(2) \quad (47)$$

Alternatively, we can algebraically solve for the parameters  $\alpha$  and  $\beta$  defining  $\mathbf{Q}$  (Eq. (8)):

$$\mathbf{M}^* = \frac{1}{\sqrt{\det(\mathbf{M})}}\mathbf{M} = \begin{bmatrix} \sigma^* & \xi^* \\ \gamma^* & \delta^* \end{bmatrix}$$

$$\tilde{\alpha} = \sigma^* + \bar{\delta}^*, \quad \tilde{\beta} = \xi^* - \bar{\gamma}^* \quad (48)$$

where  $\tilde{\alpha}, \tilde{\beta}$  are the unnormalized special unitary parameters to be normalized so  $\det(\mathbf{Q}) = 1$ .  $\alpha$  and  $\beta$  are again mapped via Eqs. (12) and (30) to a final rotation. We denote the linear algebra method **QuadMobiusSVD** and the algebraic method **QuadMobiusAlg**. Both cases assume  $\det(\mathbf{M}) \neq 0$ , and the latter assumes  $\tilde{\alpha}\bar{\tilde{\alpha}} + \tilde{\beta}\bar{\tilde{\beta}} \neq 0$ . With these maps and our assumptions (observed valid in practice), we define a full mapping from  $\Theta$  to  $\mathbf{q}$  that has a defined numerical derivative for backpropagation (see Suppl. Mat. for derivative formulas). We remark that this map is motivated by ideas from [8] and [21], inheriting many of their properties (e.g. interpretation as Bingham belief [7], differentiability [12, 24]) while offering a potentially more flexible (higher-dimensional, complex) learning representation.

## 5. Experiments

Synthetic experiments are performed to validate the proposed methods. For each trial, a ground truth quaternion rotation  $\mathbf{q}_{gt}$  is randomly sampled from  $S^3$ , and  $n$  reference points are randomly sampled from  $S^2$ . The reference points are rotated by  $\mathbf{q}_{gt}$  to obtain target observations. Gaussian noise is added to each component of each target observation, and the target observations are subsequently re-normalized afterward. Weights are randomly sampled between 0 and 1.

Accuracy is measured by the angular distance  $\theta_{err}$  in degrees between the estimated rotation  $\mathbf{q}_{est}$  and  $\mathbf{q}_{gt}$ :

$$\theta_{err} = \cos^{-1}(2(\mathbf{q}_{est} \cdot \mathbf{q}_{gt})^2 - 1) \quad (49)$$

where  $(\cdot, \cdot)$  denotes the usual vector dot product.

### 5.1. Wahba’s Problem

We first test our solutions to Wahba’s problem for both 3D and stereographic inputs (Eqs. (28) and (38)). The input for the latter is created by projecting the 3D points by  $\psi$ . We

$\epsilon_{noise}$	Q-method [3]	Ours ( $\mathbf{G}_P$ )	Ours ( $\mathbf{G}_S$ )	Ours ( $\mathbf{G}_M$ )
1e-5	1.24872e-4	1.24872e-4	1.24872e-4	3.58697e-4
0.1	1.25508	1.25508	1.25508	3.77821

Table 1. Median  $\theta_{err}$  values for Wahba’s problem with  $n = 100$ . See Suppl. Mat. for full results.

Algorithm	x	÷	√	Median $\theta_{err}$
QUEST [22]	89 / 99	1 / 1	3 / 3	9.1727 / 9.3970
Fast Quat [13]	72 / 78	3 / 3	4 / 4	9.1727 / 9.3970
Ours (Eqs. (43) and (44))	29 / 74	3 / 2	3 / 3	9.1727 / 9.3970

Table 2. Operation counts and sample result (for  $\epsilon_{noise} = 0.1$ ) for two-point solvers of Wahba’s problem. Values pairs given for unweighted/weighted algorithms without edge case handling.

also test the approximate solution in Sec. 2.3. The solutions to all three are obtained by eigendecomposition using Jacobi’s eigenvalue algorithm. For validation, we compare against several quaternion solvers introduced over the past decades. For the two-point case, we also compare against the closed-form solutions in [13] and [22]. All solutions were reimplemented and optimized similarly in C++17 and compiled with the flag `-O3`. We perform 1 million trials for each configuration and report the median  $\theta_{err}$ .

Tab. 1 confirms that our optimal solvers match the results of Davenport’s Q-method in the general case. In contrast, our Möbius approximation demonstrates a sensitivity to noise (potentially a benefit in the learning context of next section). We note that this approximation could likely be improved with a normalization step common in real homography estimation [5]. See Suppl. Mat. for full results.

Tab. 2 similarly confirms that our two-point methods achieve the same optimal results as existing solvers. By utilizing unnormalized rotations, our weighted algorithm minimizes normalization costs, streamlining the compute. Most notably, in the unweighted case, our tailored solution only requires just over a third of the multiplications of other methods, marking a significant gain in efficiency.

### 5.2. Learning Wahba’s Problem

To evaluate our rotation representations, we replicate the experiments from [8, 21, 26], using a fully-connected neural network to predict rotations aligning reference and target point inputs. Each epoch, we dynamically generate 25,600 training samples and validate on a fixed set of the same size ( $\epsilon_{noise} = 0.01$  added to all samples). We test two loss functions defined for rotation matrices:

$$1) |\mathbf{R}_{pred} - \mathbf{R}_{gt}| = \sum_i \sum_j |\mathbf{R}_{pred,i,j} - \mathbf{R}_{gt,i,j}| \quad (50)$$

$$2) \|\mathbf{R}_{pred} - \mathbf{R}_{gt}\|_F^2 \quad (51)$$

where  $\mathbf{R}_{pred}$  is the predicted rotation,  $\mathbf{R}_{gt}$  is the ground truth rotation, and  $\|\cdot\|_F$  denotes the Frobenius norm. The loss functions are referred to as **Chordal L1** and **Chordal L2** respectively. Quaternion map outputs are converted to rotation matrices for Chordal L1, while Chordal L2 is computed directly on quaternions (see [21]). The model is trained for 1000 epochs with ADAM optimizer at different learning rates, using  $n = \{3, 100\}$  and a batch size of 128. Additionally, we evaluate training complex-valued networks [1, 9] of equivalent size for the task with stereographic complex inputs (Eq. (7)). For real-valued representations, we take the real part of the model output.

We compare our rotation representations (**2-vec**, QuadMobiusAlg (**QMAlg**), and QuadMobiusSVD (**QMSVD**)) against the following other representations: **Euler** angles, quaternion (**Quat**), Gram-Schmidt (**GS**) [26], **QCQP** [21], and **SVD** [8]. Note that we used the algebraic method for the forward pass in both QuadMobius approaches to avoid an SVD computation and to isolate the differences to the backward pass formulations.

	Euler	Quat	GS	QCQP	SVD	2-vec	QMAlg	QMSVD
$\theta_{err}$	5.395	3.712	0.547	0.249	<u>0.247</u>	0.303	0.247	<b>0.242</b>
Ldr.	0	0	0	121	175	0	<b>368</b>	<u>336</u>

Table 3. Lowest error trial ( $n = 100$ , learning rate  $5e-4$ , Chordal L2 loss, real-valued) for learning Wahba’s problem.  $\theta_{err}$  is average rotation error of validation set. Second row (Ldr.) shows the number of epochs where that representation was a leader, *i.e.* had the lowest error overall as of that epoch. Bold indicates best, underline indicates second best. See Suppl. Mat. for full results.

Tab. 3 shows the trial with the lowest  $\theta_{err}$  overall (see Suppl. Mat. for complete results). As expected, the compact representations (Euler, Quat) performed relatively poorly. Overall, the best performers (QCQP, SVD, QuadMobiusAlg, QuadMobiusSVD) were all quite competitive with each other, having similar results and convergence rates. However, the QuadMobius representations together demonstrated an edge, leading most of the epochs and having the lowest error in majority of trials. Although mathematically equivalent, the two approaches produced different results with neither approach consistently outperforming the other. From these trials, it is unclear in which cases each might excel. On the other hand, 2-vec outperformed the other non-eigendecomposition representations (including Gram-Schmidt), beating them on most trials, at times by a large margin. Though it uses fewer dimensions, it still approached the top performers on many trials, providing an efficient alternative to them (see Suppl. Mat. for timings).

### 5.3. Camera Orientation Estimation

We briefly test the rotation representations on a vision task. Using images from the NERF synthetic “lego” dataset [17]



Figure 1. Sample NERF scene images used in vision task.

		Euler	Quat	GS	QCQP	SVD	2-vec	QMAlg	QMSVD
L1	Val.	7.08	5.96	4.58	4.16	4.44	<u>4.09</u>	<b>3.99</b>	4.12
	Test	12.89	6.62	5.93	4.95	5.37	<b>4.60</b>	<u>4.78</u>	5.51
L2	Val.	9.03	9.51	4.34	4.46	4.51	4.40	4.49	<b>3.96</b>
	Test	12.25	10.45	5.74	<u>5.00</u>	5.26	<b>4.81</b>	6.21	5.23

Table 4. Results of camera orientation estimation model trained with different losses (Chordal L1/L2) on NERF synthetic “lego” images. Values are average  $\theta_{err}$  for validation and test datasets. Bold indicates best value, underline indicates second best.

(Fig. 1), we learn to estimate the camera’s orientation relative to the scene (a potential initial step in NERF inversion). We apply additional random rotations to the image itself to give the ground truth rotations three degrees of freedom. Given the limited size of the dataset, images are resized to 128x128 and fed into a ShuffleNetV2-0.5 backbone [11] (initialized with pretrained ImageNet weights) followed by a single fully-connected layer featuring 50% dropout for regularization. The model is trained for 1000 epochs with ADAM optimizer, learning rate  $5e-4$ , and batch size 20.

Tab. 4 shows the results of training with both loss functions. The relative performance of different representations is mostly consistent with those of the previous experiment. The validation set results reaffirm the learning capability of the QuadMobius approaches which demonstrated on par or better performance than competing methods. Test set results however were more mixed and correlated weakly with validation results, possibly due to overfitting. Notably, our 2-vec method performed well on this task on both sets, potentially regularized by its lower-dimensionality.

## 6. Conclusion

This paper demonstrated the utility of special unitary matrices as a rotation parameterization. Several new formulas and algorithms were presented from this perspective for the real and complex domains, tackling Wahba’s problem and rotation representations in neural networks. Various experiments confirmed the potential of these approaches. Future work may include further solidifying the theoretical and empirical foundations of our rotation representations and applying special unitary matrices to other tasks such as camera pose estimation.

## References

- [1] Jose Agustin Barrachina, Chengfang Ren, Gilles Vieillard, Christele Morisseau, and Jean-Philippe Ovarlez. Theory and implementation of complex-valued neural networks, 2023. [8](#)
- [2] Daniel Choukroun. Novel results on quaternion modeling and estimation from vector observations. In *AIAA Guidance, Navigation, and Control Conference*, 2009. [5](#)
- [3] Paul B. Davenport. A vector approach to the algebra of rotations with applications. 1968. [1](#), [7](#), [17](#)
- [4] Andreas Geist, Jonas Frey, Mikel Zbrobo, Anna Levina, and Georg Martius. Learning with 3d rotations, a hitchhiker’s guide to  $so(3)$ , 2024. [1](#)
- [5] R. I. Hartley and A. Zisserman. *Multiple View Geometry in Computer Vision*. Second edition, 2004. [7](#)
- [6] Joseph B. Keller. Closest unitary, orthogonal and hermitian operators to a given operator. *Mathematics Magazine*, 48(4): 192–197, 1975. [4](#), [11](#)
- [7] John T. Kent. The complex bingham distribution and shape analysis. *Journal of the Royal Statistical Society. Series B (Methodological)*, 56(2):285–299, 1994. [7](#)
- [8] Jake Levinson, Carlos Esteves, Kefan Chen, Noah Snavely, Angjoo Kanazawa, Afshin Rostamizadeh, and Ameesh Makadia. An analysis of svd for deep rotation estimation. 2020. [1](#), [7](#), [8](#)
- [9] Xinyuan Liao. Complexnn: Complex neural network modules, 2023. [8](#)
- [10] Manolis Lourakis and George Terzakis. Efficient absolute orientation revisited. 2018. [1](#), [11](#)
- [11] Ningning Ma, Xiangyu Zhang, Hai-Tao Zheng, and Jian Sun. Shufflenet v2: Practical guidelines for efficient cnn architecture design. In *ECCV*, 2018. [8](#)
- [12] Jan R. Magnus. On differentiating eigenvalues and eigenvectors. *Econometric Theory*, 1:179 – 191, 1985. [7](#), [16](#)
- [13] F. Landis Markley. Fast quaternion attitude estimation from two vector measurements. *Journal of Guidance, Control, and Dynamics*, 25(2):411–414, 2002. [6](#), [7](#)
- [14] F. Landis Markley, Yang Cheng, John L. Crassidis, and Yaakov Oshman. Averaging quaternions. *Journal of Guidance, Control, and Dynamics*, 30(4):1193–1197, 2007. [6](#), [12](#), [13](#), [14](#)
- [15] Landis Markley. Attitude determination using vector observations and the singular value decomposition. *J. Astronaut. Sci.*, 38, 1987. [1](#), [11](#)
- [16] Landis Markley. Attitude determination using two vector measurements. 1999. [5](#)
- [17] Ben Mildenhall, Pratul P. Srinivasan, Matthew Tancik, Jonathan T. Barron, Ravi Ramamoorthi, and Ren Ng. Nerf: Representing scenes as neural radiance fields for view synthesis. In *ECCV*, 2020. [8](#)
- [18] D. Mortari. Esoq-2 single-point algorithm for fast optimal spacecraft attitude determination. 95, 1997. [1](#), [6](#), [17](#)
- [19] D. Mortari, Landis Markley, and Puneet Singla. Optimal linear attitude estimator. *Journal of Guidance, Control, and Dynamics*, 30:1619–1627, 2007. [17](#)
- [20] Caitong Peng and Daniel Choukroun. Singularity and error analysis of a simple quaternion estimator, 2024. [5](#)
- [21] Valentin Peretroukhin, Matthew Giamou, W. Greene, David Rosen, Jonathan Kelly, and Nicholas Roy. A smooth representation of belief over  $so(3)$  for deep rotation learning with uncertainty. 2020. [1](#), [6](#), [7](#), [8](#)
- [22] M. D. Shuster and S. D. Oh. Three-axis attitude determination from vector observations. *Journal of Guidance and Control*, 4(1):70–77, 1981. [1](#), [6](#), [7](#), [17](#)
- [23] Grace Wahba. A least squares estimate of satellite attitude. *SIAM Review*, 7(3):409–409, 1965. [1](#)
- [24] Zhou-Quan Wan and Shi-Xin Zhang. Automatic differentiation for complex valued svd. 2019. [7](#)
- [25] Jin Wu, Zebo Zhou, Bin Gao, Rui Li, Yuhua Cheng, and Hassen Fourati. Fast linear quaternion attitude estimator using vector observations. *IEEE Transactions on Automation Science and Engineering*, 15(1):307–319, 2018. [1](#), [17](#)
- [26] Yi Zhou, Connelly Barnes, Jingwan Lu, Jimei Yang, and Hao Li. On the continuity of rotation representations in neural networks. In *2019 IEEE/CVF Conference on Computer Vision and Pattern Recognition (CVPR)*, pages 5738–5746, 2019. [1](#), [6](#), [7](#), [8](#)

# Special Unitary Parameterized Estimators of Rotation

## Supplementary Material

### A. Proofs and Derivations

#### A.1. Proper Metric in Complex Projective Space

##### A.1.1. Derivation of Metric

Complex projective rays are equivalent if they are linearly dependent. We can test this condition by setting up the following constraint on complex vectors  $\mathbf{z} = [z_1, z_2]^T$  and  $\mathbf{p} = [p_1, p_2]^T$  for  $z_1, z_2, p_1, p_2 \in \mathbb{C}$ :

$$\det\left(\begin{bmatrix} z_1 & p_1 \\ z_2 & p_2 \end{bmatrix}\right) = z_1 p_2 - z_2 p_1 = 0$$

For vectors  $\mathbf{a} = (x_s, y_s, z_s)$ ,  $\mathbf{b} = (m_s, n_s, p_s) \in S^2$  (assume  $\mathbf{a} \neq \mathbf{p}^*$ ,  $\mathbf{b} \neq \mathbf{p}^*$ ) whose projection via  $\psi$  (Eq. (7)) correspond to  $\mathbf{z}$  and  $\mathbf{p}$  respectively, we can show that testing the linear independence of complex vectors is in fact related to the chordal distance on a sphere:

$$\begin{aligned} \lambda_1, \lambda_2 \in \mathbb{C}, \lambda_1 \neq 0, \lambda_2 \neq 0 \\ \mathbf{z} = \lambda_1 \begin{bmatrix} x_s + y_s i \\ 1 + z_s \end{bmatrix}, \mathbf{p} = \lambda_2 \begin{bmatrix} m_s + n_s i \\ 1 + p_s \end{bmatrix} \\ \det\left(\begin{bmatrix} z_1 & z_2 \\ p_1 & p_2 \end{bmatrix}\right)^2 = \end{aligned}$$

$$\begin{aligned} & |\lambda_1|^2 |\lambda_2|^2 (1 + p_s)(x_s + y_s i) - (1 + z_s)(m_s + n_s i)|^2 = \\ & |\lambda_1|^2 |\lambda_2|^2 ((1 + p_s)^2 (x_s^2 + y_s^2) + (1 + z_s)^2 (m_s^2 + n_s^2) - \\ & 2(1 + p_s)(1 + z_s)(x_s m_s + y_s n_s)) = \\ & |\lambda_1|^2 |\lambda_2|^2 (1 + p_s)(1 + z_s)((1 + p_s)(1 - z_s) + \\ & (1 + z_s)(1 - p_s) - 2(x_s m_s + y_s n_s)) = \\ & |\lambda_1|^2 |\lambda_2|^2 (1 + p_s)(1 + z_s)(2 - 2(x_s m_s + y_s n_s + z_s p_s)) \\ & = |\lambda_1|^2 |\lambda_2|^2 (1 + p_s)(1 + z_s) \|\mathbf{a} - \mathbf{b}\|^2 \end{aligned}$$

Notice that  $|\lambda_1|^2 (1 + z_s) = \frac{|z_1|^2 + |z_2|^2}{2}$  and  $|\lambda_2|^2 (1 + p_s) = \frac{|p_1|^2 + |p_2|^2}{2}$ . Substituting this into our expression and rearranging, we arrive at the final expression for the equivalent distance metric in complex projective space as:

$$\|\mathbf{a} - \mathbf{b}\|^2 = \frac{4|z_1 p_2 - z_2 p_1|^2}{(|z_1|^2 + |z_2|^2)(|p_1|^2 + |p_2|^2)}$$

The last substitution may seem unnecessary at first; however, this form is more useful as it generalizes the metric to hold even when  $\mathbf{a} = \mathbf{p}^*$  or  $\mathbf{b} = \mathbf{p}^*$  (proof below). It also gives an intuitive interpretation that the spherical chordal distance is related to a type of ‘‘cross product’’ magnitude between the two projective rays’ unit directions.

##### A.1.2. Proof of Metric for Points at Infinity

**Proposition 1** *If  $\mathbf{a} = \mathbf{p}^*$  or  $\mathbf{b} = \mathbf{p}^*$  in Eq. (20), the proper metric is still valid.*

*Proof* The squared distance of a unit length point  $\mathbf{a} = (x_s, y_s, z_s)$  to the point  $\mathbf{b} = \mathbf{p}^* = (0, 0, -1)$  is:

$$\|\mathbf{a} - \mathbf{b}\|^2 = 2 - 2\mathbf{a}^T \mathbf{b} = 2(1 + z_s)$$

Using vectors  $\mathbf{z} = \psi(\mathbf{a}) = \lambda_1[x_s + y_s i, 1 + z_s]^T$ ,  $\mathbf{p} = \psi(\mathbf{p}^*) = [\lambda_2, 0]^T$  with nonzero  $\lambda_1, \lambda_2 \in \mathbb{C}$ , for  $\mathbf{a} \neq \mathbf{p}^*$ , we can calculate the same quantity via the formula in Eq. (20):

$$\frac{4|z_1 p_2 - p_1 z_2|^2}{\|\mathbf{z}\|^2 \|\mathbf{p}\|^2} = \frac{4|\lambda_1 \lambda_2 (1 + z_s)|^2}{2|\lambda_1|^2 |\lambda_2|^2 (1 + z_s)} = 2(1 + z_s)$$

thus showing that the two formulas yield the same quantity. It is easy to see that Eq. (20) is symmetric, so the same result would hold if  $\mathbf{a} = \mathbf{p}^*$  and  $\mathbf{b} \neq \mathbf{p}^*$ . If  $\mathbf{a} = \mathbf{b} = \mathbf{p}^*$ , we can see that  $\|\mathbf{a} - \mathbf{b}\|^2$  is clearly 0. At the same time, the numerator of Eq. (20) would be 0 while the denominator is nonzero as the projective scalars  $\lambda_i \neq 0$  for any valid complex projective point. Thus, both quantities are equal in that case as well, so the formula gives the spherical chordal distance between any two points on the sphere via their stereographic projections.

#### A.2. Proof of Nearest Special Unitary Matrix

**Proposition 2** *If Möbius transformation  $\mathbf{M}$  has  $\det(\mathbf{M}) = 1$ , the nearest unitary matrix to  $\mathbf{M}$  in the Frobenius sense is special unitary.*

*Proof*  $\mathbf{M}$  has a singular value decomposition given as  $\mathbf{M} = \mathbf{U}\mathbf{\Sigma}\mathbf{V}^H$  where  $\mathbf{U}$  and  $\mathbf{V}$  are unitary matrices and  $\mathbf{\Sigma}$  is a diagonal matrix with singular values. The determinant of  $\mathbf{M}$  can be expressed as:

$$\det(\mathbf{M}) = \det(\mathbf{U})\det(\mathbf{\Sigma})\det(\mathbf{V}^H)$$

by product rule of determinants. Multiplying both sides by their complex conjugates, we obtain:

$$|\det(\mathbf{M})|^2 = |\det(\mathbf{U})|^2 |\det(\mathbf{\Sigma})|^2 |\det(\mathbf{V}^H)|^2$$

Since  $\mathbf{U}$  and  $\mathbf{V}^H$  are unitary matrices, the magnitude of their determinant is 1, so the expression simplifies to:

$$\begin{aligned} |\det(\mathbf{M})|^2 &= |\det(\mathbf{\Sigma})|^2 \\ \implies |\det(\mathbf{M})| &= |\det(\mathbf{\Sigma})| \end{aligned}$$

because the determinant magnitudes are real and nonnegative. Since  $\mathbf{\Sigma}$  is a diagonal matrix with real, nonnegative elements, its determinant is simply the product of its diagonal

entries and is in turn real and nonnegative. If  $\det(\mathbf{M}) = 1$ , then  $|\det(\boldsymbol{\Sigma})| = \det(\boldsymbol{\Sigma}) = 1$ . Coming back to the first expression, we can now write:

$$\det(\mathbf{M}) = \det(\mathbf{U})\det(\mathbf{V}^H) = \det(\mathbf{UV}^H) = 1$$

It is known that closest unitary matrix to  $\mathbf{M}$  in the Frobenius sense is the unitary part of polar decomposition [6] which can be computed by  $\mathbf{UV}^H$ . From above, we can see that  $\det(\mathbf{UV}^H) = 1$  which means that  $\mathbf{UV}^H$  is special unitary by definition.

In noiseless situations,  $\boldsymbol{\Sigma}$  is observed to be the identity matrix if  $\det(\mathbf{M}) = 1$ . As noise is added, the diagonal elements of  $\boldsymbol{\Sigma}$  drift from 1, so  $\boldsymbol{\Sigma}$  encodes a notion of how close a Möbius transformation's action is to a rotation or how much noise the problem contains, making it a candidate for optimization.

### A.3. Two Point Solutions

#### A.3.1. Proof of General Case

**Proposition 3** Let  $\mathbf{a}_i$  and  $\mathbf{b}_i$  represent the reference and target points respectively and  $\mathbf{k}_a = \mathbf{a}_1 \times \mathbf{a}_2$  and  $\mathbf{k}_b = \mathbf{b}_1 \times \mathbf{b}_2$ . For  $n = 2$  points,  $\mathbf{k}_a \neq \mathbf{0}$ , and  $\mathbf{k}_b \neq \mathbf{0}$ , the optimal rotation to Wahba's problem is given as the weighted average (in the Frobenius sense) between two rotations  $\mathbf{R}_1$  and  $\mathbf{R}_2$  defined by  $\mathbf{R}_i \mathbf{a}_i = \mathbf{b}_i$  and  $\mathbf{R}_i \frac{\mathbf{k}_a}{\|\mathbf{k}_a\|} = \frac{\mathbf{k}_b}{\|\mathbf{k}_b\|}$ .

*Lemma:* If all points lie in the plane  $z=0$  and  $\mathbf{k}_a \neq \mathbf{0}$ ,  $\mathbf{k}_b \neq \mathbf{0}$ , and  $\mathbf{k}_a \cdot \mathbf{k}_b > 0$ , the optimal rotation is a rotation around the  $z$ -axis.

Since all points lie in the plane  $z = 0$ , the last column and row of  $\mathbf{B}$  (Eq. (2)) are zero. As a result, the last column and row of  $\mathbf{BB}^T$  and  $\mathbf{B}^T\mathbf{B}$  are also zero, so they both have a kernel vector of  $(0, 0, 1)$ . For the SVD of  $\mathbf{B}$  given as  $\mathbf{U}\boldsymbol{\Sigma}\mathbf{V}^T$ , the optimal rotation  $\mathbf{R}$  (via [15]) can take the form:

$$\mathbf{R} = \begin{bmatrix} \cdot & \cdot & 0 \\ \cdot & \cdot & 0 \\ 0 & 0 & 1 \end{bmatrix} \begin{bmatrix} 1 & 0 & 0 \\ 0 & 1 & 0 \\ 0 & 0 & \det(\mathbf{U})\det(\mathbf{V}) \end{bmatrix} \begin{bmatrix} \cdot & \cdot & 0 \\ \cdot & \cdot & 0 \\ 0 & 0 & 1 \end{bmatrix}$$

where  $\det(\mathbf{U})\det(\mathbf{V})$  is either 1 or -1 since  $\mathbf{U}$  and  $\mathbf{V}$  are orthogonal matrices. Thus, the last column and row of  $\mathbf{R}$  are both  $(0, 0, 1)$  or  $(0, 0, -1)$ . In order for  $\mathbf{R}$  to be a valid rotation matrix, the remaining upper 2x2 submatrix must be an orthogonal matrix which can be generated by a single parameter  $\theta$ . Furthermore, the sign of the bottom right corner element of  $\mathbf{R}$  must be the same as the determinant of the upper 2x2 submatrix for  $\det(\mathbf{R}) = 1$ . These conditions reduce  $\mathbf{R}$  to one of the two general forms:

$$\begin{bmatrix} \cos(\theta_1) & -\sin(\theta_1) & 0 \\ \sin(\theta_1) & \cos(\theta_1) & 0 \\ 0 & 0 & 1 \end{bmatrix}, \begin{bmatrix} \cos(\theta_2) & \sin(\theta_2) & 0 \\ \sin(\theta_2) & -\cos(\theta_2) & 0 \\ 0 & 0 & -1 \end{bmatrix}$$

We denote the former as  $\mathbf{R}_{SO}$  and the latter as  $\mathbf{R}_O$ . The optimal solution to Wahba's problem maximizes the gain

function  $Tr(\mathbf{R}\mathbf{B}^T)$  [10]. This quantity for both forms can be expressed as below:

$$\begin{aligned} Tr(\mathbf{R}_{SO}\mathbf{B}^T) &= \lambda_{1,1}\cos(\theta_1) + \lambda_{1,2}\sin(\theta_1) \\ Tr(\mathbf{R}_O\mathbf{B}^T) &= \lambda_{2,1}\cos(\theta_2) + \lambda_{2,2}\sin(\theta_2) \\ \lambda_{1,1} &= \mathbf{B}_{1,1} + \mathbf{B}_{2,2}, \quad \lambda_{1,2} = \mathbf{B}_{2,1} - \mathbf{B}_{1,2} \\ \lambda_{2,1} &= \mathbf{B}_{1,1} - \mathbf{B}_{2,2}, \quad \lambda_{2,2} = \mathbf{B}_{2,1} + \mathbf{B}_{1,2} \end{aligned}$$

The gain function in both cases is the dot product between  $(\lambda_{i,1}, \lambda_{i,2})$  and  $(\cos(\theta_i), \sin(\theta_i))$ . Its maximum value (subject to the constraint  $\cos(\theta_i)^2 + \sin(\theta_i)^2 = 1$ ) is obtained by the unit vector aligned with  $(\lambda_{i,1}, \lambda_{i,2})$ , i.e.:

$$\cos(\theta_i) = \frac{\lambda_{i,1}}{\sqrt{\lambda_{i,1}^2 + \lambda_{i,2}^2}}, \quad \sin(\theta_i) = \frac{\lambda_{i,2}}{\sqrt{\lambda_{i,1}^2 + \lambda_{i,2}^2}}$$

Substituting this back into the gain function, we see that the optimal value is simply the magnitude of  $(\lambda_{i,1}, \lambda_{i,2})$ :

$$\begin{aligned} Tr(\mathbf{R}_{SO}\mathbf{B}^T) &= \sqrt{\lambda_{1,1}^2 + \lambda_{1,2}^2} \\ Tr(\mathbf{R}_O\mathbf{B}^T) &= \sqrt{\lambda_{2,1}^2 + \lambda_{2,2}^2} \end{aligned}$$

Since the square root function is monotonically increasing, the larger of the two radicands corresponds to the larger gain value. We can compare them directly by taking their difference:

$$\begin{aligned} &(\lambda_{1,1}^2 + \lambda_{1,2}^2) - (\lambda_{2,1}^2 + \lambda_{2,2}^2) \\ &= 4w_1w_2(\mathbf{k}_a \cdot \mathbf{k}_b) \end{aligned}$$

where  $w_i$  are the weights. Since the weights are positive and the cross products are assumed nonzero, the quantity above is positive when  $\mathbf{k}_a$  and  $\mathbf{k}_b$  point in the same direction and negative otherwise. Thus, when the cross products of the reference and target sets are aligned,  $\mathbf{R}_{SO}$  corresponds to the larger gain value and is the optimal rotation. It takes the form of a rotation about the  $z$ -axis. ■

*Proof* We assume that all points lie in the plane  $z = 0$  and that the cross product of the reference and target sets are nonzero and are aligned. This will be generalized later. We construct rotations  $\mathbf{R}_1$  and  $\mathbf{R}_2$  to be rotations about the  $z$ -axis that align  $\mathbf{a}_1$  to  $\mathbf{b}_1$  and  $\mathbf{a}_2$  to  $\mathbf{b}_2$  respectively. Since the input points have unit length and the vector norm is rotationally invariant, we can rewrite the loss function as:

$$\begin{aligned} &w_1\|\mathbf{b}_1 - \mathbf{R}\mathbf{a}_1\|^2 + w_2\|\mathbf{b}_2 - \mathbf{R}\mathbf{a}_2\|^2 \\ &= w_1\|\mathbf{a}_1 - \mathbf{R}_1^T\mathbf{R}\mathbf{a}_1\|^2 + w_2\|\mathbf{a}_2 - \mathbf{R}_2^T\mathbf{R}\mathbf{a}_2\|^2 \\ &= w_1\|(\mathbf{I} - \mathbf{R}_1^T\mathbf{R})\mathbf{a}_1\|^2 + w_2\|(\mathbf{I} - \mathbf{R}_2^T\mathbf{R})\mathbf{a}_2\|^2 \\ &= w_1\mathbf{a}_1^T(\mathbf{I} - \mathbf{R}_1^T\mathbf{R})^T(\mathbf{I} - \mathbf{R}_1^T\mathbf{R})\mathbf{a}_1 \\ &\quad + w_2\mathbf{a}_2^T(\mathbf{I} - \mathbf{R}_2^T\mathbf{R})^T(\mathbf{I} - \mathbf{R}_2^T\mathbf{R})\mathbf{a}_2 \\ &= 2(w_1 + w_2) - 2w_1\mathbf{a}_1^T\mathbf{R}_1^T\mathbf{R}\mathbf{a}_1 - 2w_2\mathbf{a}_2^T\mathbf{R}_2^T\mathbf{R}\mathbf{a}_2 \end{aligned}$$

using the fact  $\mathbf{a}_i^T \mathbf{R}_i^T \mathbf{R}_a \mathbf{a}_i = \mathbf{a}_i^T \mathbf{R}^T \mathbf{R}_i \mathbf{a}_i$ . Under our assumptions, the lemma establishes that the optimal rotation  $\mathbf{R}$  is a rotation about the z-axis. Since both  $\mathbf{R}_1$  and  $\mathbf{R}_2$  are also rotations about the z-axis, we can easily verify that the products  $\mathbf{R}_1^T \mathbf{R}$  and  $\mathbf{R}_2^T \mathbf{R}$  are rotations about the z-axis as well. Using Rodrigues' rotation formula, we can expand the term below as follows:

$$\begin{aligned} & \mathbf{a}_1^T \mathbf{R}_1^T \mathbf{R} \mathbf{a}_1 = \\ & \mathbf{a}_1 \cdot (\cos(\phi) \mathbf{a}_1 + \sin(\phi) \mathbf{k} \times \mathbf{a}_1 + (1 - \cos(\phi)) (\mathbf{k} \cdot \mathbf{a}_1) \mathbf{k}) \\ & = \cos(\phi) + \sin(\phi) (\mathbf{a}_1 \cdot (\mathbf{k} \times \mathbf{a}_1)) = \cos(\phi) \end{aligned}$$

where  $\phi$  is the angle of rotation of  $\mathbf{R}_1^T \mathbf{R}$  and  $\mathbf{k} = [0, 0, 1]^T$  is the axis of rotation. The simple result is due to the fact that  $\mathbf{a}_1$  is orthogonal to the axis of rotation and has unit length. On the other hand, we note that the Frobenius norm between  $\mathbf{R}_1$  and  $\mathbf{R}$  computes the following:

$$\begin{aligned} \|\mathbf{R}_1 - \mathbf{R}\|_F^2 &= \text{Tr}((\mathbf{R}_1 - \mathbf{R})^T (\mathbf{R}_1 - \mathbf{R})) \\ &= 6 - 2\text{Tr}(\mathbf{R}_1^T \mathbf{R}) \\ &= 6 - 2\text{Tr}(\cos(\phi) \mathbf{I} + \sin(\phi) [\mathbf{k}]_{\times} + (1 - \cos(\phi)) \mathbf{k} \mathbf{k}^T) \\ &= 6 - 6\cos(\phi) - 2(1 - \cos(\phi)) = 4 - 4\cos(\phi) \\ \cos(\phi) &= 1 - \frac{1}{4} \|\mathbf{R}_1 - \mathbf{R}\|_F^2 \end{aligned}$$

The expansion of  $\mathbf{R}_1^T \mathbf{R}$  above is due to the axis-angle formula for rotation matrices where  $[\mathbf{k}]_{\times}$  denotes the traceless skew-symmetric matrix formed from  $\mathbf{k}$  representing a vector cross product. Deriving a similar result for  $\mathbf{a}_2^T \mathbf{R}_2^T \mathbf{R} \mathbf{a}_2$  and plugging both back into our reformulated loss function, we can rewrite it as:

$$\begin{aligned} & 2(w_1 + w_2) - 2w_1 \left(1 - \frac{1}{4} \|\mathbf{R}_1 - \mathbf{R}\|_F^2\right) \\ & \quad - 2w_2 \left(1 - \frac{1}{4} \|\mathbf{R}_2 - \mathbf{R}\|_F^2\right) \\ & = \frac{1}{2} w_1 \|\mathbf{R}_1 - \mathbf{R}\|_F^2 + \frac{1}{2} w_2 \|\mathbf{R}_2 - \mathbf{R}\|_F^2 \end{aligned}$$

Through this expression, we can see that the rotation  $\mathbf{R}$  which minimized our original loss is exactly the rotation that represents the weighted average in the Frobenius sense between  $\mathbf{R}_1$  and  $\mathbf{R}_2$  as specified in [14]. The uniform factor of  $\frac{1}{2}$  is irrelevant to the optimization.

Now we generalize the result. Starting from the assumed configuration, we can extend it to general configurations by applying arbitrary rotations  $\mathbf{R}_a$  and  $\mathbf{R}_b$  to the reference and target points respectively, transforming them into  $\mathbf{a}'_i$  and  $\mathbf{b}'_i$ . In this new coordinate frame, the rotation matrix  $\mathbf{R}'$  is re-

lated to the original optimal matrix  $\mathbf{R}$  as shown below:

$$\begin{aligned} & \sum_i w_i \|\mathbf{b}_i - \mathbf{R} \mathbf{a}_i\|^2 \\ & = \sum_i w_i \|\mathbf{R}_b \mathbf{b}_i - \mathbf{R}_b \mathbf{R} \mathbf{a}_i\|^2 \\ & = \sum_i w_i \|\mathbf{R}_b \mathbf{b}_i - \mathbf{R}_b \mathbf{R} (\mathbf{R}_a^T \mathbf{R}_a) \mathbf{a}_i\|^2 \\ & = \sum_i w_i \|\mathbf{b}'_i - (\mathbf{R}_b \mathbf{R} \mathbf{R}_a^T) \mathbf{a}'_i\|^2 \\ & \quad \mathbf{R}' = \mathbf{R}_b \mathbf{R} \mathbf{R}_a^T \end{aligned}$$

Because the vector norm is invariant under rotation, the optimal loss value remains unchanged across all coordinate frames. Since the optimal value from the original coordinate frame is preserved above,  $\mathbf{R}'$  represents the optimal rotation in the new frame. Furthermore, the Frobenius norm is also rotation-invariant, so we can apply the required rotations to estimate  $\mathbf{R}'$  as follows:

$$\begin{aligned} \sum_i w_i \|\mathbf{R}_i - \mathbf{R}\|_F^2 &= \sum_i w_i \|\mathbf{R}_b \mathbf{R}_i \mathbf{R}_a^T - \mathbf{R}_b \mathbf{R} \mathbf{R}_a^T\|_F^2 \\ &= \sum_i w_i \|\mathbf{R}_b \mathbf{R}_i \mathbf{R}_a^T - \mathbf{R}'\|_F^2 \\ \mathbf{R}'_1 &= \mathbf{R}_b \mathbf{R}_1 \mathbf{R}_a^T, \quad \mathbf{R}'_2 = \mathbf{R}_b \mathbf{R}_2 \mathbf{R}_a^T \end{aligned}$$

Thus, in the general case, the optimal rotation is given by the weighted average rotation between  $\mathbf{R}'_1$  and  $\mathbf{R}'_2$ . We can uniquely identify those rotations with at least two linearly independent points they transform. Starting with the reference and target sets:

$$\begin{aligned} \mathbf{R}_i \mathbf{a}_i &\equiv \mathbf{b}_i \\ \mathbf{R}_b \mathbf{R}_i (\mathbf{R}_a^T \mathbf{R}_a) \mathbf{a}_i &= \mathbf{R}_b \mathbf{b}_i \\ \mathbf{R}'_i \mathbf{a}'_i &= \mathbf{b}'_i \end{aligned}$$

Each rotation still aligns their respective reference point to their target point. Furthermore, in our original coordinate frame,  $\mathbf{k}_a$  and  $\mathbf{k}_b$  are aligned and are parallel or antiparallel to  $\mathbf{R}_i$ 's axis of rotation (z-axis), so they are unchanged by  $\mathbf{R}_i$ . As a result:

$$\begin{aligned} \mathbf{R}_i \frac{\mathbf{k}_a}{\|\mathbf{k}_a\|} &= \frac{\mathbf{k}_b}{\|\mathbf{k}_b\|} \\ \mathbf{R}_b \mathbf{R}_i (\mathbf{R}_a^T \mathbf{R}_a) \frac{\mathbf{k}_a}{\|\mathbf{k}_a\|} &= \mathbf{R}_b \frac{\mathbf{k}_b}{\|\mathbf{k}_b\|} \\ \mathbf{R}'_i \frac{\mathbf{R}_a (\mathbf{a}_1 \times \mathbf{a}_2)}{\|\mathbf{R}_a (\mathbf{a}_1 \times \mathbf{a}_2)\|} &= \frac{\mathbf{R}_b (\mathbf{b}_1 \times \mathbf{b}_2)}{\|\mathbf{R}_b (\mathbf{b}_1 \times \mathbf{b}_2)\|} \\ \mathbf{R}'_i \frac{\mathbf{a}'_1 \times \mathbf{a}'_2}{\|\mathbf{a}'_1 \times \mathbf{a}'_2\|} &= \frac{\mathbf{b}'_1 \times \mathbf{b}'_2}{\|\mathbf{b}'_1 \times \mathbf{b}'_2\|} \end{aligned}$$

due to rotations distributing over the cross product. Thus, we can identify  $\mathbf{R}'_1$  and  $\mathbf{R}'_2$  as the rotations that align their

corresponding reference point to their target point along with the cross products of the reference and target sets. As the cross products are assumed nonzero and are orthogonal to their respective point set, the two points aligned by each rotation are always independent and therefore uniquely define the rotations. As shown, the optimal rotation is the weighted average in the Frobenius sense between them.

### A.3.2. Proof of Unweighted Case

**Proposition 4** *Let  $\mathbf{a}_i$ ,  $\mathbf{b}_i$ , and  $w_i$  represent the reference points, target points, and weights respectively. Given  $n = 2$  points,  $w_1 = w_2$ ,  $\mathbf{a}_1 \times \mathbf{a}_2 \neq \mathbf{0}$ , and  $\mathbf{b}_1 \times \mathbf{b}_2 \neq \mathbf{0}$ , the optimal rotation to Wahba's problem is given by the unique rotation  $\mathbf{R}$  defined by  $\mathbf{R}(\frac{\mathbf{a}_1 + \mathbf{a}_2}{\|\mathbf{a}_1 + \mathbf{a}_2\|}) = \frac{\mathbf{b}_1 + \mathbf{b}_2}{\|\mathbf{b}_1 + \mathbf{b}_2\|}$  and  $\mathbf{R}(\frac{\mathbf{a}_1 - \mathbf{a}_2}{\|\mathbf{a}_1 - \mathbf{a}_2\|}) = \frac{\mathbf{b}_1 - \mathbf{b}_2}{\|\mathbf{b}_1 - \mathbf{b}_2\|}$ .*

*Proof* For two 3D unit vectors  $\mathbf{v}_1$  and  $\mathbf{v}_2$ , we introduce the following notation and easily verifiable results:

$$\begin{aligned}\tilde{\mathbf{v}}^- &\equiv \mathbf{v}_1 - \mathbf{v}_2, \quad \tilde{\mathbf{v}}^+ \equiv \mathbf{v}_1 + \mathbf{v}_2 \\ \mathbf{v}^- &= \frac{\tilde{\mathbf{v}}^-}{\|\tilde{\mathbf{v}}^-\|}, \quad \mathbf{v}^+ = \frac{\tilde{\mathbf{v}}^+}{\|\tilde{\mathbf{v}}^+\|} \\ \tilde{\mathbf{v}}^- \cdot \tilde{\mathbf{v}}^+ &= 0 \\ \mathbf{v}_1 \cdot \tilde{\mathbf{v}}^+ &= \mathbf{v}_2 \cdot \tilde{\mathbf{v}}^+ \\ \tilde{\mathbf{v}}^- \times \tilde{\mathbf{v}}^+ &= 2(\mathbf{v}_1 \times \mathbf{v}_2) \\ \mathbf{v}_1 \times \mathbf{v}_2 \neq \mathbf{0} &\implies \tilde{\mathbf{v}}^- \neq \mathbf{0}, \tilde{\mathbf{v}}^+ \neq \mathbf{0}\end{aligned}$$

If  $\mathbf{v}_1 \times \mathbf{v}_2 \neq \mathbf{0}$ , then the two vectors  $\mathbf{v}^-$  and  $\mathbf{v}^+$  are well-defined and form an orthonormal basis for the plane spanned by  $\mathbf{v}_1$  and  $\mathbf{v}_2$ . Consequently,  $\mathbf{v}^-$  and  $\mathbf{v}^+$  created from one pair of linearly independent unit vectors can be perfectly aligned with those created from another pair.

With  $\mathbf{a}_1 \times \mathbf{a}_2 \neq \mathbf{0}$ ,  $\mathbf{b}_1 \times \mathbf{b}_2 \neq \mathbf{0}$ , we initially assume that the points are configured such that they all lie in the plane  $z = 0$  and that  $\mathbf{a}^+ = \mathbf{b}^+$  and  $\mathbf{a}^- = \mathbf{b}^-$ . This is generalized later. For this configuration, we note the following:

$$\begin{aligned}\mathbf{a}_1 \times \mathbf{a}_2 &= \frac{1}{2}(\tilde{\mathbf{a}}^- \times \tilde{\mathbf{a}}^+) \\ &= \frac{1}{2}\|\tilde{\mathbf{a}}^-\|\|\tilde{\mathbf{a}}^+\|(\mathbf{a}^- \times \mathbf{a}^+) = \frac{1}{2}\|\tilde{\mathbf{a}}^-\|\|\tilde{\mathbf{a}}^+\|(\mathbf{b}^- \times \mathbf{b}^+) \\ &= \frac{\|\tilde{\mathbf{a}}^-\|\|\tilde{\mathbf{a}}^+\|}{2\|\tilde{\mathbf{b}}^-\|\|\tilde{\mathbf{b}}^+\|}(\mathbf{b}^- \times \mathbf{b}^+) = \frac{\|\tilde{\mathbf{a}}^-\|\|\tilde{\mathbf{a}}^+\|}{\|\tilde{\mathbf{b}}^-\|\|\tilde{\mathbf{b}}^+\|}(\mathbf{b}_1 \times \mathbf{b}_2) \\ &\implies (\mathbf{a}_1 \times \mathbf{a}_2) \cdot (\mathbf{b}_1 \times \mathbf{b}_2) > 0\end{aligned}$$

Thus, the cross products are aligned in this configuration, and from the lemma in the general case proof, the optimal rotation is a rotation about the z-axis.

From the dot product equality above, we can deduce that  $\mathbf{a}^+$  is equidistant from  $\mathbf{a}_1, \mathbf{a}_2$ . The dot product calculates the cosine of the angle between linearly independent unit vectors measured in the plane spanned by the vectors ( $z = 0$  in our case). We know from the proof in the general case

that the dot product of a unit vector in the plane  $z = 0$  with itself after a rotation about the z-axis is the cosine of the angle of rotation. That angle is measured in the plane perpendicular to the axis of rotation, which is also the plane  $z = 0$ . Thus, constructing rotations  $\mathbf{R}_{\mathbf{a}_1}$  and  $\mathbf{R}_{\mathbf{a}_2}$  which rotate  $\mathbf{a}^+$  about the z-axis to  $\mathbf{a}_1$  and  $\mathbf{a}_2$  respectively, we can write the following:

$$\begin{aligned}\mathbf{a}_1 \cdot \mathbf{a}^+ &= \mathbf{a}_2 \cdot \mathbf{a}^+ \\ &= \mathbf{a}^+ \cdot (\mathbf{R}_{\mathbf{a}_1} \mathbf{a}^+) = \mathbf{a}^+ \cdot (\mathbf{R}_{\mathbf{a}_2} \mathbf{a}^+) = \cos(\phi)\end{aligned}$$

where  $\phi$  denotes the angle of rotation of  $\mathbf{R}_{\mathbf{a}_1}$ , making  $|\phi|$  (canonically positive) the angle between  $\mathbf{a}_1$  and  $\mathbf{a}^+$ . In general,  $\mathbf{R}_{\mathbf{a}_1} \neq \mathbf{R}_{\mathbf{a}_2}$ , otherwise  $\mathbf{a}_1$  and  $\mathbf{a}_2$  would be identical. In order for the above to still hold, the angle of rotation of  $\mathbf{R}_{\mathbf{a}_2}$  must have the same magnitude but opposite sign of  $\phi$ . A similar statement can be made for the target points.

Let  $\mathbf{R}_{\mathbf{b}_1}$  and  $\mathbf{R}_{\mathbf{b}_2}$  represent rotations about the z-axis that align  $\mathbf{b}^+$  with  $\mathbf{b}_1$  and  $\mathbf{b}_2$  respectively. Recall  $\mathbf{a}^+ = \mathbf{b}^+$ . We construct the rotations  $\mathbf{R}_1 = \mathbf{R}_{\mathbf{b}_1} \mathbf{R}_{\mathbf{a}_1}^T$  and  $\mathbf{R}_2 = \mathbf{R}_{\mathbf{b}_2} \mathbf{R}_{\mathbf{a}_2}^T$  which are also about the z-axis to align  $\mathbf{a}_1$  with  $\mathbf{b}_1$  and  $\mathbf{a}_2$  with  $\mathbf{b}_2$  respectively. If  $\psi$  is the rotation angle of  $\mathbf{R}_{\mathbf{b}_1}$ , then the angle of rotation for  $\mathbf{R}_1$  is  $-\phi + \psi$  since  $\mathbf{R}_{\mathbf{a}_1}$  and  $\mathbf{R}_{\mathbf{b}_1}$  share the same axis of rotation and transposing a rotation matrix negates the rotation angle. For  $\mathbf{R}_2$ , the rotation angle is  $\phi - \psi$ , as  $\mathbf{R}_{\mathbf{a}_2}$  rotates by  $-\phi$  and  $\mathbf{R}_{\mathbf{b}_2}$  by  $-\psi$ . Thus, the rotation angles of  $\mathbf{R}_1$  and  $\mathbf{R}_2$  have equal magnitudes but opposite signs.

From the proof in the general case, the optimal rotation  $\mathbf{R}$  is the weighted average in the Frobenius sense between the rotations  $\mathbf{R}_1$  and  $\mathbf{R}_2$  recently constructed. The weighted average rotation maximizes the quantity  $Tr(\mathbf{R}\mathbf{B}'^T)$  where  $\mathbf{B}' = \sum_i w_i \mathbf{R}_i$  [14]. Given the previously made statements and the fact that  $w_1 = w_2$ , we can calculate  $\mathbf{B}'$  as:

$$\begin{aligned}\mathbf{R}_1 &= \begin{bmatrix} \cos(-\phi + \psi) & -\sin(-\phi + \psi) & 0 \\ \sin(-\phi + \psi) & \cos(-\phi + \psi) & 0 \\ 0 & 0 & 1 \end{bmatrix}, \\ \mathbf{R}_2 &= \begin{bmatrix} \cos(\phi - \psi) & -\sin(\phi - \psi) & 0 \\ \sin(\phi - \psi) & \cos(\phi - \psi) & 0 \\ 0 & 0 & 1 \end{bmatrix}, \\ \mathbf{B}' &= w_1 \mathbf{R}_1 + w_2 \mathbf{R}_2 \\ &= 2w_1 \begin{bmatrix} \cos(-\phi + \psi) & 0 & 0 \\ 0 & \cos(-\phi + \psi) & 0 \\ 0 & 0 & 1 \end{bmatrix}\end{aligned}$$

due to the fact that sine is an odd function and cosine is an even function. Since  $\mathbf{R}$  is a rotation about the z-axis, we can directly compute  $Tr(\mathbf{R}\mathbf{B}'^T)$  as  $2w_1(2\cos(-\phi + \psi)\cos(\theta) + 1)$  where  $\theta$  is  $\mathbf{R}$ 's angle of rotation. We can trivially see that  $\theta$  must take on a value of 0 or  $\pi$  (mod  $2\pi$ ) to be optimal, depending on the sign of  $\cos(-\phi + \psi)$  as  $w_1$  is positive. That sign can be determined considering  $\mathbf{a}^-$  and  $\mathbf{b}^-$  are

aligned:

$$\begin{aligned}
& \tilde{\mathbf{a}}^- \cdot \tilde{\mathbf{b}}^- > 0 \\
& (\mathbf{R}_{\mathbf{a}_1} \mathbf{a}^+ - \mathbf{R}_{\mathbf{a}_2} \mathbf{a}^+) \cdot (\mathbf{R}_{\mathbf{b}_1} \mathbf{b}^+ - \mathbf{R}_{\mathbf{b}_2} \mathbf{b}^+) > 0 \\
& \mathbf{a}^+ \cdot ((\mathbf{R}_{\mathbf{a}_1} - \mathbf{R}_{\mathbf{a}_2})^T (\mathbf{R}_{\mathbf{b}_1} - \mathbf{R}_{\mathbf{b}_2}) \mathbf{a}^+) > 0 \\
& \quad \cos(-\phi + \psi) - \cos(-\phi - \psi) \\
& \quad -\cos(\phi + \psi) + \cos(\phi - \psi) > 0 \\
& 2\cos(-\phi + \psi) - 2\cos(\phi + \psi) > 0
\end{aligned}$$

Since  $\mathbf{a}^+$  and  $\mathbf{b}^+$  are also aligned, we can similarly derive  $2\cos(-\phi + \psi) + 2\cos(\phi + \psi) > 0$ . Adding both inequalities together (valid since they are positive quantities), we find that  $\cos(-\phi + \psi) > 0$ . Thus,  $\theta$  must be 0 to maximize  $Tr(\mathbf{R}\mathbf{B}'^T)$ , resulting in  $\mathbf{R}$  being the identity matrix and indicating that the current alignment is the optimal one.

To generalize this, we again apply arbitrary rotations  $\mathbf{R}_a, \mathbf{R}_b$  to the reference and target sets respectively, transforming them into  $\mathbf{a}'_i, \mathbf{b}'_i$ . From the proof in the general case, the new optimal rotation  $\mathbf{R}' = \mathbf{R}_b \mathbf{R} \mathbf{R}_a^T = \mathbf{R}_b \mathbf{R}_a^T$ . Now, we simply verify below that this rotation aligns  $\mathbf{a}'^+$  to  $\mathbf{b}'^+$  and  $\mathbf{a}'^-$  to  $\mathbf{b}'^-$  (combined  $\pm$  notation for convenience):

$$\begin{aligned}
\mathbf{a}^\pm &= \mathbf{b}^\pm = \frac{\mathbf{a}_1 \pm \mathbf{a}_2}{\|\mathbf{a}_1 \pm \mathbf{a}_2\|} = \frac{\mathbf{b}_1 \pm \mathbf{b}_2}{\|\mathbf{b}_1 \pm \mathbf{b}_2\|} \\
\frac{\mathbf{R}_b(\mathbf{a}_1 \pm \mathbf{a}_2)}{\|\mathbf{a}_1 \pm \mathbf{a}_2\|} &= \frac{\mathbf{b}'_1 \pm \mathbf{b}'_2}{\|\mathbf{b}'_1 \pm \mathbf{b}'_2\|} \\
\frac{\mathbf{R}_b \mathbf{R}_a^T (\mathbf{a}'_1 \pm \mathbf{a}'_2)}{\|\mathbf{a}'_1 \pm \mathbf{a}'_2\|} &= \frac{\mathbf{b}'_1 \pm \mathbf{b}'_2}{\|\mathbf{b}'_1 \pm \mathbf{b}'_2\|} \\
\mathbf{R}' \mathbf{a}'^\pm &= \mathbf{b}'^\pm
\end{aligned}$$

Since  $\mathbf{a}'^+$  and  $\mathbf{a}'^-$  are orthogonal, they are also linearly independent, and their transformation uniquely defines the rotation  $\mathbf{R}'$ , thereby completing the proof.

### A.3.3. Average of Two Unnormalized Quaternions

In [14], it was shown that the average rotation matrix in the Frobenius sense can be calculated via the quaternion  $\mathbf{q}$  which optimizes the following:

$$\begin{aligned}
\mathbf{M} &= \sum_i w_i \mathbf{q}_i \mathbf{q}_i^T \\
\max_{\mathbf{q}} \mathbf{q}^T \mathbf{M} \mathbf{q} \quad s.t. \quad \|\mathbf{q}\| &= 1
\end{aligned}$$

Where  $\mathbf{q}_i$  are the unit norm quaternions corresponding to the rotations being averaged (sign of  $\mathbf{q}_i$  is irrelevant). The solution is the eigenvector corresponding to the largest eigenvalue of  $\mathbf{M}$ . In the two point approach to Wahba's problem proposed previously, we need to construct two quaternion rotations and average them. The formulation above assumes all quaternions have unit norm. However, it would be computationally advantageous (see Tab. 2) if we did not have to normalize the constructed rotations,

thereby avoiding two square root and division operations. From [14], it is known that the average rotation in the two rotation case is simply a linear combination of the rotations being averaged. To average unnormalized quaternions  $\tilde{\mathbf{q}}_1$  and  $\tilde{\mathbf{q}}_2$ , we can express  $\mathbf{M}$  and  $\mathbf{q}$  as:

$$\begin{aligned}
\mathbf{M} &= w_1 \frac{\|\tilde{\mathbf{q}}_2\|^2}{\|\tilde{\mathbf{q}}_1\|^2} \tilde{\mathbf{q}}_1 \tilde{\mathbf{q}}_1^T + w_2 \tilde{\mathbf{q}}_2 \tilde{\mathbf{q}}_2^T \\
\mathbf{q} &= \mu \tilde{\mathbf{q}}_1 + \nu \tilde{\mathbf{q}}_2
\end{aligned}$$

where  $\mu, \nu$  are scalars. The above takes advantage of the fact that scaling  $\mathbf{M}$  does not change its eigenvectors. Thus, we reduce the problem from estimating a unit quaternion to estimating two scalars. As a result, we can rewrite the objective as:

$$\begin{aligned}
\mathbf{\Gamma} &= \begin{bmatrix} \|\tilde{\mathbf{q}}_1\|^2 & \tilde{\mathbf{q}}_1 \cdot \tilde{\mathbf{q}}_2 \\ \tilde{\mathbf{q}}_1 \cdot \tilde{\mathbf{q}}_2 & \|\tilde{\mathbf{q}}_2\|^2 \end{bmatrix}, \quad \mathbf{v} = \begin{bmatrix} \mu \\ \nu \end{bmatrix} \\
\mathbf{\Lambda}_{1,1} &= w_1 \|\tilde{\mathbf{q}}_1\|^2 \|\tilde{\mathbf{q}}_2\|^2 + w_2 (\tilde{\mathbf{q}}_1 \cdot \tilde{\mathbf{q}}_2)^2 \\
\mathbf{\Lambda}_{1,2} &= \mathbf{\Lambda}_{2,1} = (w_1 + w_2) \|\tilde{\mathbf{q}}_2\|^2 (\tilde{\mathbf{q}}_1 \cdot \tilde{\mathbf{q}}_2) \\
\mathbf{\Lambda}_{2,2} &= \|\tilde{\mathbf{q}}_2\|^2 \left( w_2 \|\tilde{\mathbf{q}}_2\|^2 + \frac{w_1 (\tilde{\mathbf{q}}_1 \cdot \tilde{\mathbf{q}}_2)^2}{\|\tilde{\mathbf{q}}_1\|^2} \right) \\
\max_{\mathbf{v}} \mathbf{v}^T \mathbf{\Lambda} \mathbf{v} \quad s.t. \quad \mathbf{v}^T \mathbf{\Gamma} \mathbf{v} &= 1
\end{aligned}$$

where  $\cdot$  denotes the usual vector dot product.  $\mathbf{\Gamma}$  is the quadratic constraint ensuring that the linear combination of  $\tilde{\mathbf{q}}_1$  and  $\tilde{\mathbf{q}}_2$  has unit norm, and  $\mathbf{\Lambda}$  is the new 2x2 objective to optimize over. Using the method of Lagrange multipliers, we find that the solution to the above takes the form of a generalized eigenvalue problem  $\mathbf{\Lambda} \mathbf{v} = \lambda \mathbf{\Gamma} \mathbf{v}$ . Note that the scaling constraint  $\mathbf{\Gamma}$  is positive semidefinite, generally representing the equation of an ellipse. Assuming  $\mathbf{\Gamma}$  is invertible and well-conditioned (it is discussed later when this is not the case), the solution is the eigenvector of  $\mathbf{\Gamma}^{-1} \mathbf{\Lambda}$  corresponding to the largest eigenvalue. Through simplification and scaling, we can express the matrix similarly as:

$$\mathbf{\Gamma}^{-1} \mathbf{\Lambda} \sim \begin{bmatrix} w_1 \|\tilde{\mathbf{q}}_1\|^2 \|\tilde{\mathbf{q}}_2\|^2 & w_1 \|\tilde{\mathbf{q}}_2\|^2 (\tilde{\mathbf{q}}_1 \cdot \tilde{\mathbf{q}}_2) \\ w_2 \|\tilde{\mathbf{q}}_1\|^2 (\tilde{\mathbf{q}}_1 \cdot \tilde{\mathbf{q}}_2) & w_2 \|\tilde{\mathbf{q}}_1\|^2 \|\tilde{\mathbf{q}}_2\|^2 \end{bmatrix}$$

which maintains its eigenvectors from before. Since the matrix is only 2x2, the eigenvector  $\mathbf{v}$  corresponding to the largest eigenvalue can be expressed in closed form. Scaling the eigenvector by the constraint  $\mathbf{v}^T \mathbf{\Gamma} \mathbf{v} = 1$  and substituting it back into the original linear combination of  $\tilde{\mathbf{q}}_1$  and  $\tilde{\mathbf{q}}_2$ , we obtain the average quaternion as:

$$\mathbf{q} = \frac{\mu \tilde{\mathbf{q}}_1 + \nu \tilde{\mathbf{q}}_2}{\sqrt{\|\tilde{\mathbf{q}}_1\|^2 \mu^2 + \|\tilde{\mathbf{q}}_2\|^2 \nu^2 + 2(\tilde{\mathbf{q}}_1 \cdot \tilde{\mathbf{q}}_2) \mu \nu}}$$

where the values  $\mu$  and  $\nu$  can be expressed equivalently in two ways:

$$\begin{aligned}\tau^{(1)} &= (w_1 - w_2) \|\tilde{\mathbf{q}}_1\|^2 \|\tilde{\mathbf{q}}_2\|^2, \\ \omega^{(1)} &= 2w_1 \|\tilde{\mathbf{q}}_2\|^2 (\tilde{\mathbf{q}}_1 \cdot \tilde{\mathbf{q}}_2) \\ \nu^{(1)} &= 2w_2 \|\tilde{\mathbf{q}}_1\|^2 (\tilde{\mathbf{q}}_1 \cdot \tilde{\mathbf{q}}_2) \\ \mu^{(1)} &= \tau^{(1)} + \sqrt{(\tau^{(1)})^2 + \omega^{(1)}\nu^{(1)}}\end{aligned}$$

or

$$\begin{aligned}\tau^{(2)} &= (w_2 - w_1) \|\tilde{\mathbf{q}}_1\|^2 \|\tilde{\mathbf{q}}_2\|^2, \\ \omega^{(2)} &= 2w_2 \|\tilde{\mathbf{q}}_1\|^2 (\tilde{\mathbf{q}}_1 \cdot \tilde{\mathbf{q}}_2) \\ \mu^{(2)} &= 2w_1 \|\tilde{\mathbf{q}}_2\|^2 (\tilde{\mathbf{q}}_1 \cdot \tilde{\mathbf{q}}_2) \\ \nu^{(2)} &= \tau^{(2)} + \sqrt{(\tau^{(2)})^2 + \omega^{(2)}\mu^{(2)}}\end{aligned}$$

Both yield the same result except when  $\tilde{\mathbf{q}}_1 \cdot \tilde{\mathbf{q}}_2 = 0$  in which case the rotation corresponding to the larger weight is chosen. If  $w_1 = w_2$  in that case, then there is no unique solution and either of the rotations can be selected. The former solution set is used when  $w_1 > w_2$  and the latter is used when  $w_1 \leq w_2$  as to approach the correct value as  $\tilde{\mathbf{q}}_1 \cdot \tilde{\mathbf{q}}_2 \rightarrow 0$ .

Note that the denominator in the expression for the average quaternion is simply  $\sqrt{\mathbf{v}^T \mathbf{\Gamma} \mathbf{v}}$ . Previously,  $\mathbf{\Gamma}$  was assumed non-singular and well-conditioned, but there are two cases in practice where this fails to hold. The first is when  $\tilde{\mathbf{q}}_1$  and  $\tilde{\mathbf{q}}_2$  are linearly dependent, i.e. they represent the same rotation. If we choose the solution constants above by the previously described strategy and examine the expressions for  $\mu$  and  $\nu$ , then it can be seen that  $\mathbf{v}^T \mathbf{\Gamma} \mathbf{v}$  is in fact strictly positive for nontrivial solutions  $\mathbf{v}$  and nonzero weights/magnitudes. Furthermore, it can also be seen that  $\mu \tilde{\mathbf{q}}_1$  and  $\nu \tilde{\mathbf{q}}_2$  share the same direction in this case and thus cannot cancel out. The second case occurs when the magnitudes of  $\tilde{\mathbf{q}}_1$  and/or  $\tilde{\mathbf{q}}_2$  are small, causing  $\mathbf{\Gamma}$  to be ill-conditioned. This case can be avoided by using the strategy described in Sec. 3.2 to only obtain quaternions of sufficient magnitude or by simply scaling/normalizing the rotations when necessary.

#### A.3.4. Degenerate Case Solution

The degenerate case occurs when either of the cross products of the reference or target points vanish, and the previous approaches for the two point case cannot be applied. This is because the solution is no longer unique. A particular one can be efficiently found through the following approach.

We assume without loss of generality that the target points are collinear (the reference points may or may not be) and the first target point is aligned with the x-axis (i.e.  $\mathbf{b}_1 = (1, 0, 0)$ ). In this case, the last two columns of the

constraint  $\mathbf{C}_i$  (Eq. (36)) vanish. We can thus write our optimization as:

$$\begin{aligned}\mathbf{C}_i &= \begin{bmatrix} (m-x)i & y-zi \\ -y-zi & (x+m)i \end{bmatrix}, \quad \mathbf{u} = \begin{bmatrix} \alpha \\ \beta \end{bmatrix} \\ \mathbf{Z} &= \sum_i w_i \mathbf{C}_i^H \mathbf{C}_i \\ \min_{\mathbf{u}} \mathbf{u}^H \mathbf{Z} \mathbf{u} \quad s.t. \quad \mathbf{u}^H \mathbf{u} &= 1\end{aligned}$$

This optimization is simpler than before and can now be solved directly over the special unitary parameters. Since  $\mathbf{Z}$  is Hermitian and positive semidefinite, the solution is the complex eigenvector of  $\mathbf{Z}$  corresponding to the smallest eigenvalue. For reference points  $\mathbf{a}_i = (x_i, y_i, z_i)$ , this can be expressed in closed form as:

$$\tilde{\mathbf{u}} = \begin{bmatrix} w_1 x_1 + w_2 x_2 + \|w_1 \mathbf{a}_1 + w_2 \mathbf{a}_2\| \\ w_1 z_1 + w_2 z_2 - (w_1 y_1 + w_2 y_2) i \end{bmatrix}$$

or

$$\tilde{\mathbf{u}} = \begin{bmatrix} w_1 x_1 - w_2 x_2 + \|w_1 \mathbf{a}_1 - w_2 \mathbf{a}_2\| \\ w_1 z_1 - w_2 z_2 - (w_1 y_1 - w_2 y_2) i \end{bmatrix}$$

where  $\tilde{\mathbf{u}}$  is the unnormalized eigenvector and the correct solution depends on the target points' configuration. If the dot product of the target points is positive, then the first expression is correct. Otherwise, the second is correct. Note that eigenvectors are only unique up to scale, so even after normalizing the solution so that  $\mathbf{u}^H \mathbf{u} = 1$ , we can still apply an arbitrary unitary scaling of  $e^{i\theta}$ . This corresponds to a rotation about the x-axis and parameterizes the family of optimal solutions.

For arbitrary collinear target points, we simply need to find any rotation aligning the x-axis to the first target point  $\mathbf{b}_1$  and then compose it with  $\mathbf{u}$ . If the reference points were collinear instead, we can swap the reference and target points in the above approach and invert the rotation afterwards. In practice, we would choose the more degenerate (i.e. larger dot product magnitude) of the two sets to treat as collinear.

Examining the solution closer, it can be seen that  $\mathbf{u}$  represents a rotation aligning a weighted combination of the reference points we refer to as the "weighted average" with the x-axis. The weighted average takes the form of a sum ( $w_1 \mathbf{a}_1 + w_2 \mathbf{a}_2$ ) or difference ( $w_1 \mathbf{a}_1 - w_2 \mathbf{a}_2$ ) depending on the sign of the dot product between target points. This suggests that a more straightforward approach in practice would be to simply calculate the normalized weighted average of the reference points and align it with  $\mathbf{b}_1$  directly. This generalizes to the case when the reference points are collinear similarly to before. If the weighted average is zero, then any rotation is optimal.

## B. Backpropagation Derivatives

For a simple complex square matrix  $\mathbf{G}$ , the derivative of an eigenvector  $\mathbf{v}$  of  $\mathbf{G}$  with respect to the elements of  $\mathbf{G}$  can be computed as [12]:

$$d\mathbf{v} = (\lambda\mathbf{I} - \mathbf{G})^+ \left( \mathbf{I} - \frac{\mathbf{v}\mathbf{v}^H}{\mathbf{v}^H\mathbf{v}} \right) (d\mathbf{G})\mathbf{v}$$

where  $\lambda$  is the eigenvalue corresponding to  $\mathbf{v}$ ,  $\mathbf{I}$  is the identity matrix, and  $^+$  denotes the Moore-Penrose pseudoinverse. Typically,  $\mathbf{v}^H\mathbf{v} = 1$  by convention for most eigenvector solvers. In our original problem (Eq. (32)),  $\mathbf{G}_M$  is Hermitian as opposed to a general matrix, so the elements of  $\Theta$  are repeated in the matrix through conjugation. Using complex differentiation conventions consistent with many deep learning frameworks, the loss derivative can be written as:

$$\frac{d\mathcal{L}}{d(\mathbf{G}_M)_{i,j}} = \frac{1}{2} \left( \left\langle \frac{d\mathbf{v}}{d\mathbf{G}_{i,j}}, \frac{d\mathcal{L}}{d\mathbf{v}} \right\rangle + \left\langle \frac{d\mathcal{L}}{d\mathbf{v}}, \frac{d\mathbf{v}}{d\mathbf{G}_{j,i}} \right\rangle \right)$$

where  $\langle \cdot, \cdot \rangle$  denotes the complex inner product and  $\mathcal{L}$  is the scalar loss.  $\frac{d\mathcal{L}}{d\Theta}$  can be extracted from the upper triangular portion of  $\frac{d\mathcal{L}}{d\mathbf{G}_M}$  (after reshaping to 4 x 4), multiplying by 2 for the off-diagonal parameters to include the lower portion contribution. This method avoids the need for the other eigenvectors or eigenvalues of  $\mathbf{G}_M$  that weren't used in the forward pass.

For QuadMobiusSVD (Eq. (47)), the backpropagation must go through the SVD operation  $\mathbf{M} = \mathbf{U}\Sigma\mathbf{V}^H$ . It is well known that the nearest unitary matrix, calculated as  $\mathbf{U}\mathbf{V}^H$ , corresponds to the unitary component  $\mathbf{Q}$  of the polar decomposition of  $\mathbf{M} = \mathbf{Q}\mathbf{P}$ , where  $\mathbf{P}$  is a positive semidefinite and Hermitian matrix. Thus, instead of backpropagating through SVD, we can backpropagate directly through  $\mathbf{Q}$  (assuming  $\mathbf{M}$  has full-rank) in a more direct way utilizing the SVD forward pass elements (derivation omitted):

$$\mathbf{S} = \text{diag}(\Sigma) \oplus \text{diag}(\Sigma)$$

$$d\mathbf{Q} = \mathbf{U} \left( \frac{\mathbf{U}^H(d\mathbf{M})\mathbf{V} - \mathbf{V}^H(d\mathbf{M}^H)\mathbf{U}}{\mathbf{S}} \right) \mathbf{V}^H$$

where  $\oplus$  denotes an outer sum operation, and the division is Hadamard division (element-wise). From this equation, the numerical complex derivative can be calculated and simplified to the following (note the indices,  $\mathbf{F}$  is 2 x 2 x 2 x 2):

$$\mathbf{F}_{j,m,l,k} = \mathbf{U}_{j,k}(\mathbf{V}^H)_{l,m}$$

$$\frac{d\mathcal{L}}{d\mathbf{M}_{j,m}} = \left\langle \mathbf{U} \left( \frac{\mathbf{F}_{j,m}^H}{\mathbf{S}} \right) \mathbf{V}^H, \frac{d\mathcal{L}}{d\mathbf{Q}} \right\rangle_F - \left\langle \frac{d\mathcal{L}}{d\mathbf{Q}}, \mathbf{U} \left( \frac{\mathbf{F}_{j,m}}{\mathbf{S}} \right) \mathbf{V}^H \right\rangle_F$$

where  $\langle \cdot, \cdot \rangle_F$  denotes the complex Frobenius inner product.

The remaining operations in the maps are algebraically straightforward to differentiate through. We observe that the previous formulas compute the same gradients as PyTorch's automatic differentiation through complex functions `torch.linalg.eigh` and `torch.linalg.svd`.

## C. General Stereographic Constraint

The generalized constraint between complex rays  $[z_1, z_2]^T$  and  $[p_1, p_2]^T$  where  $z_1 = x_1 + y_1i$ ,  $z_2 = x_2 + y_2i$ ,  $p_1 = m_1 + n_1i$ , and  $p_2 = m_2 + n_2i$  is given by:

$$w'_i = \frac{4w_i}{(|z_1|^2 + |z_2|^2)(|p_1|^2 + |p_2|^2)}$$

$$\mathbf{A}_i\mathbf{u} = \begin{bmatrix} -z_1p_2 & -z_2p_2 & p_1z_2 & -p_1z_1 \end{bmatrix} \mathbf{u} = 0$$

for complex inputs and below for real inputs:

$$\mathbf{D}_{i,0} = \begin{bmatrix} m_2x_1 - m_1x_2 + n_1y_2 - n_2y_1 \\ m_2y_1 - m_1y_2 + n_2x_1 - n_1x_2 \end{bmatrix}$$

$$\mathbf{D}_{i,1} = \begin{bmatrix} -m_2y_1 - m_1y_2 - n_2x_1 - n_1x_2 \\ m_2x_1 + m_1x_2 - n_1y_2 - n_2y_1 \end{bmatrix}$$

$$\mathbf{D}_{i,2} = \begin{bmatrix} m_1x_1 + m_2x_2 - n_1y_1 - n_2y_2 \\ m_1y_1 + m_2y_2 + n_1x_1 + n_2x_2 \end{bmatrix}$$

$$\mathbf{D}_{i,3} = \begin{bmatrix} m_1y_1 - m_2y_2 + n_1x_1 - n_2x_2 \\ m_2x_2 - m_1x_1 + n_1y_1 - n_2y_2 \end{bmatrix}$$

$$\mathbf{D}_i\mathbf{q} = [\mathbf{D}_{i,0} \quad \mathbf{D}_{i,1} \quad \mathbf{D}_{i,2} \quad \mathbf{D}_{i,3}] \mathbf{q} = 0$$

We can verify that with  $z_2 = 1$  and  $p_2 = 1$ , we obtain the original results in Eq. (25) and Eq. (27). Furthermore, we can use  $z_2 = 0$  and  $p_2 = 0$  to calculate results involving the projective point at infinity. Thus, there are no singularities using the general constraint. From this, we can derive similar formulas and algorithms for the one and two point cases as those proposed earlier.

Similarly, the following is the general constraint for estimating a Möbius transformation from stereographic inputs:

$$\mathbf{A}'_i\mathbf{m} = \begin{bmatrix} -z_1p_2 & -z_2p_2 & p_1z_1 & p_1z_2 \end{bmatrix} \mathbf{m} = 0$$

## D. Remark on Connection with Hopf Fibration

The set of rotations aligning the unit vector  $\mathbf{a}$  to  $\mathbf{b}$  is described by the kernel of  $\mathbf{Q}_i$  (Eq. (37)). Geometrically, the kernel defines a 2D plane through the origin in 4D space, and its intersection with  $S^3$  (representing unit quaternions) forms a great circle. This great circle provides a linear algebra parametrization of an  $S^1$  fiber whose image under the Hopf map (for canonical choice of  $\mathbf{a}$ ) is the point  $\mathbf{b}$  on  $S^2$ . A classical description of the fibration is seen in *Sec. A.3.4* when  $\mathbf{u}$  is interpreted as the map's image in  $\mathbb{C}\mathbb{P}^1$ . The fiber associated with  $\mathbf{u}$  is thus parameterized by the scalar  $e^{i\theta}$ .

## E. Additional Experiment Data

(See following pages)

Algorithm	$n = 3$				$n = 100$			
	$\epsilon_{noise}=1e-5$	$\epsilon_{noise}=1e-3$	$\epsilon_{noise}=0.1$	Timings	$\epsilon_{noise}=1e-5$	$\epsilon_{noise}=1e-3$	$\epsilon_{noise}=0.1$	Timings
Q-method [3]	7.4676e-4	7.4678e-2	7.4868	3.583	1.2487e-4	1.2487e-2	1.2551	5.375
QUEST [22]	7.4676e-4	7.4678e-2	7.4868	0.250	1.2487e-4	1.2487e-2	1.2551	1.875
ESOQ2 [18]	7.4694e-4	7.4691e-2	7.4869	0.375	1.2487e-4	1.2487e-2	1.2551	2.000
FLAE [25]	7.4676e-4	7.4678e-2	7.4868	0.333	1.2487e-4	1.2487e-2	1.2551	1.875
OLAE [19]	7.7118e-4	7.7138e-2	7.8639	0.208	1.3120e-4	1.3145e-2	1.5952	2.167
Ours ( $G_P$ , Eq. (28))	7.4676e-4	7.4678e-2	7.4868	4.084	1.2487e-4	1.2487e-2	1.2551	9.917
Ours ( $G_S$ , Eq. (38))	7.4676e-4	7.4678e-2	7.4868	3.625	1.2487e-4	1.2487e-2	1.2551	6.500
Ours ( $G_M$ , Eq. (32))	1.2614e-3	1.2613e-1	12.608	0.917	3.5870e-4	3.5871e-2	3.7782	41.875

Table 5. Complete results of various Wahba’s Problem solvers against varying noise levels with  $n = \{3, 100\}$ . Accuracy values reported are median  $\theta_{err}$ , and timing values are median runtimes in microseconds. Timings taken with  $\epsilon_{noise}=0.1$ . See Sec. 5.1 for more info.

#	$n$	LR	Loss	Domain	Euler	Quat	GS	QCQP	SVD	2-vec	QMAlg	QMSVD
1	3	1e-4	L2	Real	9.009 / 0	8.964 / 1	1.761 / 0	1.676 / <u>141</u>	<b>1.641 / 696</b>	1.701 / 1	<u>1.658 / 51</u>	1.689 / 110
2	3	1e-4	L2	Complex	119.364 / 0	13.632 / 0	5.768 / 0	4.237 / 1	4.264 / 1	5.781 / 0	<u>3.823 / 109</u>	<b>3.761 / 889</b>
3	3	5e-4	L2	Real	12.154 / 0	9.618 / 0	1.583 / 5	1.518 / 143	<b>1.491 / 582</b>	1.560 / 0	<u>1.501 / 217</u>	1.527 / 53
4	3	5e-4	L2	Complex	119.403 / 0	12.238 / 0	4.016 / 0	3.586 / 2	3.735 / 6	3.917 / 0	<u>3.447 / 751</u>	<b>3.408 / 241</b>
5	3	1e-3	L2	Real	14.693 / 0	9.159 / 0	1.575 / 1	<u>1.497 / 170</u>	1.509 / <u>245</u>	1.578 / 2	<b>1.486 / 87</b>	1.499 / <b>495</b>
6	3	1e-3	L2	Complex	119.397 / 0	11.212 / 0	3.290 / 24	3.289 / 190	3.253 / <b>384</b>	3.269 / 0	<u>3.250 / 110</u>	<b>3.232 / 292</b>
7	3	1e-4	L1	Real	8.063 / 0	4.120 / 0	1.603 / 0	<u>1.445 / 135</u>	<b>1.421 / 622</b>	1.570 / 2	1.469 / <u>164</u>	1.459 / 77
8	3	1e-4	L1	Complex	119.388 / 0	9.812 / 0	4.734 / 0	3.259 / 0	3.238 / 1	4.663 / 0	<u>2.835 / 492</u>	<b>2.786 / 507</b>
9	3	5e-4	L1	Real	8.687 / 0	4.355 / 0	1.459 / 0	1.315 / 175	1.322 / <u>279</u>	1.416 / 0	<b>1.303 / 418</b>	<u>1.306 / 128</u>
10	3	5e-4	L1	Complex	119.334 / 0	7.500 / 0	3.290 / 0	<u>2.760 / 3</u>	2.857 / 3	3.113 / 0	<b>2.750 / 921</b>	<u>2.807 / 73</u>
11	3	1e-3	L1	Real	10.833 / 0	4.436 / 0	1.434 / 0	1.312 / 53	<u>1.301 / 338</u>	1.427 / 0	1.317 / <u>337</u>	<b>1.291 / 272</b>
12	3	1e-3	L1	Complex	119.483 / 0	6.930 / 0	2.916 / 0	2.475 / 92	<b>2.447 / 251</b>	2.874 / 0	2.478 / 211	<u>2.472 / 446</u>
13	100	1e-4	L2	Real	3.784 / 0	3.277 / 0	0.569 / 0	0.253 / 138	<b>0.243 / 389</b>	0.313 / 0	0.255 / 169	<u>0.251 / 304</u>
14	100	1e-4	L2	Complex	48.175 / 0	4.988 / 0	1.400 / 0	0.638 / 254	0.637 / 136	0.850 / 0	<b>0.625 / 281</b>	<u>0.634 / 329</u>
15	100	5e-4	L2	Real	5.395 / 0	3.712 / 0	0.547 / 0	0.249 / 121	<u>0.247 / 175</u>	0.303 / 0	0.247 / <b>368</b>	<b>0.242 / 336</b>
16	100	5e-4	L2	Complex	119.370 / 0	5.009 / 0	1.586 / 0	<b>0.831 / 682</b>	0.866 / <u>223</u>	0.940 / 0	0.866 / 66	<u>0.848 / 29</u>
17	100	1e-3	L2	Real	6.608 / 0	3.269 / 0	0.537 / 0	<b>0.243 / 292</b>	0.272 / 112	0.297 / 0	0.261 / <b>299</b>	<u>0.253 / 297</u>
18	100	1e-3	L2	Complex	118.381 / 0	5.056 / 0	1.480 / 0	0.845 / 121	<u>0.836 / 499</u>	0.887 / 0	0.859 / 71	<b>0.826 / 309</b>
19	100	1e-4	L1	Real	2.249 / 0	1.794 / 0	0.356 / 0	0.269 / <u>293</u>	<b>0.261 / 327</b>	0.332 / 0	0.264 / 130	0.265 / 250
20	100	1e-4	L1	Complex	109.217 / 0	3.209 / 0	0.927 / 0	<b>0.665 / 268</b>	<u>0.667 / 469</u>	0.889 / 0	0.669 / 196	0.669 / 67
21	100	5e-4	L1	Real	2.666 / 0	1.055 / 0	0.355 / 0	<u>0.275 / 83</u>	0.284 / <u>339</u>	0.316 / 1	0.289 / 209	<b>0.272 / 368</b>
22	100	5e-4	L1	Complex	119.299 / 0	1.954 / 0	0.938 / 0	0.883 / <b>780</b>	<u>0.877 / 101</u>	0.956 / 0	<b>0.873 / 73</b>	0.878 / 46
23	100	1e-3	L1	Real	3.867 / 0	1.384 / 0	0.366 / 0	<u>0.280 / 167</u>	0.280 / <u>316</u>	0.331 / 0	<b>0.277 / 346</b>	0.291 / 171
24	100	1e-3	L1	Complex	83.623 / 0	2.184 / 0	0.952 / 0	<u>0.830 / 466</u>	0.835 / 61	0.919 / 0	<b>0.826 / 366</b>	0.849 / 107

Table 6. Trial results for learning Wahba’s problem with different rotation representations.  $n$  is number of points, LR is learning rate, Loss is type of chordal loss function, Domain is whether network is real-valued or complex-valued. Results are shown as  $\theta_{err}/Ldr.$  pairs where  $\theta_{err}$  is average rotation error on validation set, and Ldr. is the number of epochs where that representation was a leader, *i.e.* had the lowest  $\theta_{err}$  overall as of that epoch. Bold indicates best value, underline indicates second best. See Sec. 5.2 for more info. Remarks: Some of the complex-valued trials featured the highest leader rates overall by our representations (*e.g.* trial #2, trial #10).

	Euler	Quaternion	Gram-Schmidt	QCQP	SVD	2-vec	QuadMobiusAlg	QuadMobiusSVD
Training	0.2123	0.0691	0.4903	0.5223	0.4904	0.4447	1.2231	1.6247
Inference	0.0401	0.0056	0.1050	0.2435	0.2737	0.0803	0.4298	0.6221

Table 7. Comparison of timings of different representations run with batch size 128. Measured on Apple M1 Silicon CPU. Values reported are median measurements of 10000 runs in milliseconds. Training includes forward and backward passes (PyTorch train mode), and Inference includes only forward pass (PyTorch eval mode). Remarks: 2-vec has notably fast inference timings. QuadMobius representations are slower than others as they involve complex arithmetic and more compute steps overall. However, training time differences were observed to be negligible between them and QCQP/SVD as bottlenecks are typically present elsewhere in the pipeline (*e.g.* data loading, network compute).

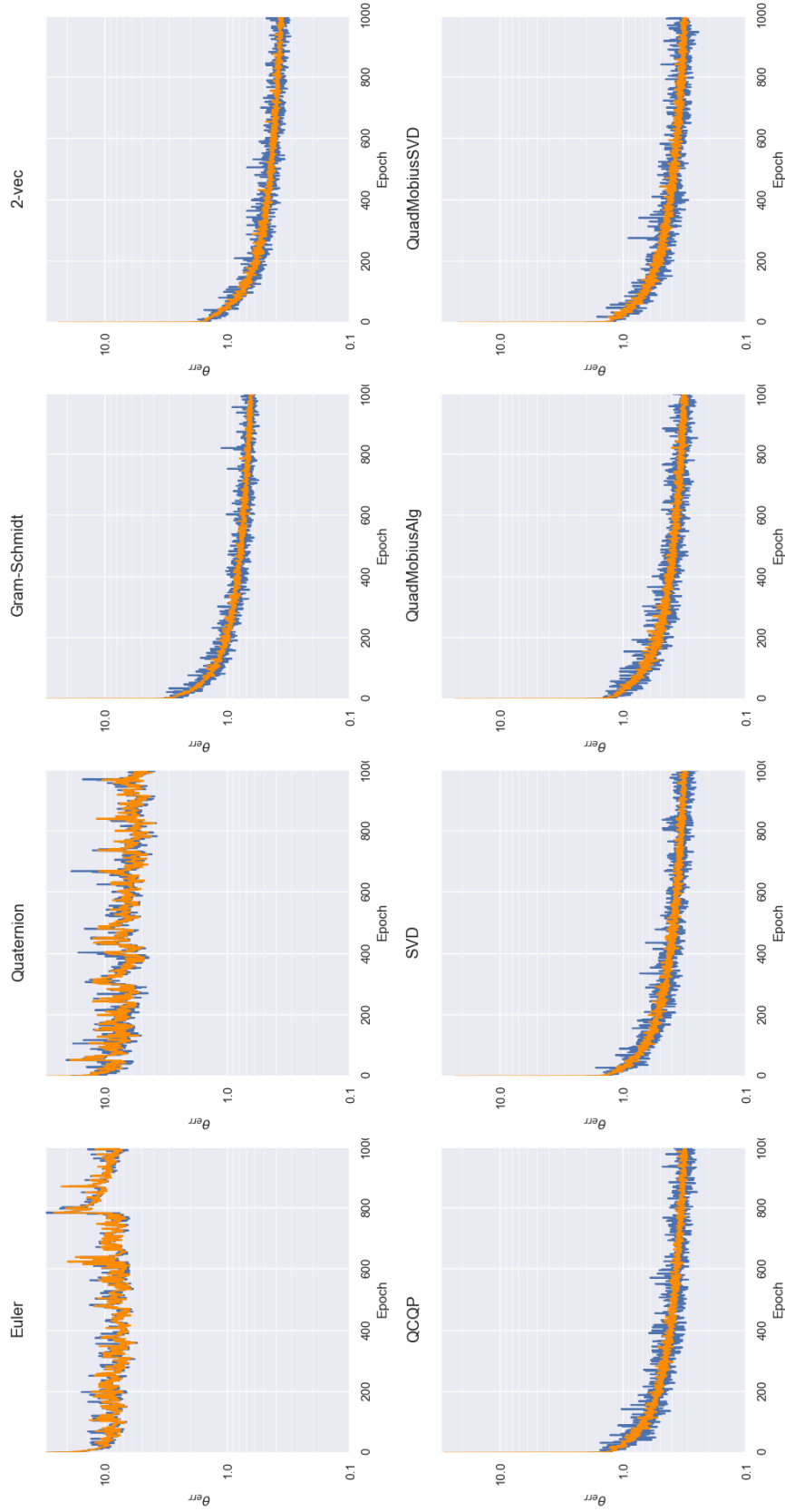


Figure 2. Progression of average  $\theta_{err}$  over the train and validation sets for learning Wahba's problem (Sec. 5.2) for the trial with lowest average  $\theta_{err}$  overall (trial #15 in Tab. 6). Orange is training, blue is validation. Remarks: Note the significant difference between 2-vec and Gram-Schmidt, the competitiveness of the top four representations, and the stability in training for parameterizations in 6D or higher.